

Mechanical and biological consequences of repetitive loading: crack initiation and fatigue failure in the red macroalga *Mazzaella*

Katharine J. Mach

Hopkins Marine Station of Stanford University, Pacific Grove, CA 93950, USA

e-mail: mach@stanford.edu

Accepted 15 January 2009

SUMMARY

On rocky shores, wave-swept macroalgae experience dramatic and repeated wave-induced hydrodynamic forces. However, previous studies of macroalgal mechanics have shown that individual waves are not forceful enough to account for observed rates of breakage. Instead, fatigue may contribute to algal breakage, with damage accumulating over time in conditions of repeated loading. Here I examine the entire process of fatigue, from crack initiation to eventual specimen fracture, in the common red alga *Mazzaella*. Propensity for fatigue failure in laboratory tests varied with life history phase and species: at a given repeated loading stress, male gametophytes endured more loading cycles before breakage than tetrasporophytes, which in turn lasted longer than female gametophytes; likewise, *M. splendens* withstood more loading cycles at a given repeated loading stress than *M. flaccida*. Fatigue failure begins with formation of cracks, the timing and location of which were assessed. Cracks formed, on average, after approximately 80–90% of cycles required for failure had passed, although crack timing varied with life history phase. Also, crack formation frequently occurred in association with endophytes and female gametophyte reproductive structures, suggesting a cost of endophyte infection and a tradeoff between reproduction and mechanical survival. Comparison between laboratory and field loading conditions provides robust confirmation that fatigue breaks fronds in natural *M. flaccida* populations. Large, female gametophyte fronds are predicted to be most susceptible to fatigue failure in the field, whereas small, male gametophyte fronds are least likely to break.

Key words: fatigue, crack initiation, crack growth, breakage, life history phases, endophytes, *Mazzaella*, macroalgae, seaweed, biomechanics.

INTRODUCTION

Seaweeds densely populate many rocky intertidal shores, a physically stringent environment presenting terrestrial stressors at low tide and buffeting by breaking waves at high tide. When tides are low, seaweeds experience desiccation, wide temperature fluctuations and increased sunlight (Denny and Wethey, 2001; Tomanek and Helmuth, 2002). Alternately, when tides are high, water velocities imposed by waves frequently reach 5–10 m s⁻¹ and even exceed 35 m s⁻¹ at times (Gaylord, 1999; Denny and Gaylord, 2002) (M. L. Boller and M. W. Denny, personal communication). Intertidal macroalgae, tethered to the shore, experience substantial hydrodynamic forces, primarily as drag (Gaylord et al., 1994; Gaylord, 2000; Boller and Carrington, 2006a). Furthermore, waves strike shores approximately every 10 s and thus exert forces on seaweeds regularly and repeatedly over entire algal lifetimes.

Unsurprisingly, intertidal seaweeds break frequently in this harsh fluid environment (Seymour et al., 1989; Dudgeon and Johnson, 1992; Dudgeon et al., 1999; Johnson, 2001; Pratt and Johnson, 2002). Wintertime reductions in algal populations frequently exceed 10–90% for intertidal macroalgae (e.g. Hansen and Doyle, 1976; Hansen, 1977; Foster, 1982; Dudgeon and Johnson, 1992; Dyck and DeWreede, 1995; Dyck and DeWreede, 2006a; Dyck and DeWreede, 2006b) and span from 2% to 94% for offshore kelp (Seymour et al., 1989). A few general terms for seaweed morphology will aid discussion of this breakage. A macroalga adheres to the substratum through a holdfast, from which emerges one or several fronds. For seaweeds examined in this study, each frond consists of a stem-like stipe and a flattened blade, which may bear reproductive structures. Holdfast and

frond(s) together constitute the seaweed's thallus. Macroalgal breakage assumes a variety of forms, with some species' fronds tattering marginally (Black, 1976; Blanchette, 1997; Dudgeon et al., 1999), other species' thalli breaking in the middle of blades or at holdfast–stipe junctions (Carrington, 1990; Hawes and Smith, 1995; Shaughnessy et al., 1996; Shaughnessy and DeWreede, 2001; Carrington et al., 2001; Johnson, 2001), and still other species commonly dislodging due to holdfast or substratum failure (Black, 1976; Koehl, 1986; Seymour et al., 1989; Utter and Denny, 1996; Gaylord and Denny, 1997). For most seaweeds, such breakage ultimately results in the death of dislodged portions of algal thalli.

Biomechanical studies have largely failed to identify mechanisms that account for this frequent algal breakage. In the traditional biomechanical approach, researchers have measured macroalgal breaking strengths by extending specimens to failure. They then have compared these strengths with maximum drag forces exerted on seaweeds in the field (Koehl and Alberte, 1988; Gaylord et al., 1994; Gaylord, 2000; Johnson and Koehl, 1994; Friedland and Denny, 1995; Utter and Denny, 1996; Denny et al., 1997; Johnson, 2001; Kitzes and Denny, 2005). Such examinations predict that seaweeds only infrequently experience isolated wave forces sufficient to cause breakage in this pull-to-break manner. In other words, high observed rates of breakage and dislodgment cannot be explained on the basis of maximum wave-imposed forces alone.

Researchers have thus suggested other explanations for algal breakage, scenarios in which isolated waves may break seaweeds with compromised strength. For example, intertidal macroalgae

may break only when previously damaged by herbivory or abrasion, when weakened by senescence or physiological low-tide stressors, or when entangled with other algae (Friedland and Denny, 1995; Utter and Denny, 1996; Kitzes and Denny, 2005; Denny, 2006), although data on such mechanisms of breakage are lacking.

Alternatively, macroalgae may break by fatigue (Koehl, 1984; Koehl, 1986; Hale, 2001; Kitzes and Denny, 2005; Mach et al., 2007a; Mach et al., 2007b). Even when stresses applied to a material never exceed the material's pull-to-break strength, the material (seaweed or otherwise) still may break due to gradual weakening. In conditions of repeated loading, fatigue leads to failure through a two-part process. First, microscopic cracks appear, originating from material defects or other regions of concentrated stress. Then, fatigue loading elongates initial cracks incrementally until they are long enough to propagate rapidly and cause complete fracture. The relative durations of crack initiation and fatigue crack growth vary in different materials. In some cases, cracks form easily but often cease growing upon encountering barriers to their propagation (O'Brien et al., 2003; Taylor et al., 2007). In other cases, cracks form less frequently but, once formed, grow more readily to the point of fracture (Stephens et al., 2001).

Seaweeds, which experience repeated wave-induced stresses, may accumulate fatigue damage that leads to the eventual fracture of algal thalli. In explorations of macroalgal fatigue, Hale (Hale, 2001) and Mach and colleagues (Mach et al., 2007a; Mach et al., 2007b) employed techniques from the engineering field of fracture mechanics to quantify fatigue growth of cracks introduced into algal blades. Mach and colleagues extrapolated this quantified crack growth to algal blades without introduced cracks, tentatively predicting that the entire process of fatigue operates on time scales relevant to macroalgal breakage in the field.

However, full understanding of fatigue failure requires knowledge of the role and mechanism of crack initiation, as well as of fatigue crack growth and final fracture. Formation of cracks has been monitored in biological materials such as bone and dentin (Ziopoulos and Currey, 1994; Ziopoulos et al., 1996; Nalla et al., 2003; O'Brien et al., 2003; Taylor et al., 2007), but crack initiation has been little explored in soft biological materials [but see Ker for discussion of cracks in tendon (Ker, 2007)]. Flat macroalgal blades provide unique soft biological tissue in which crack initiation can be continually, easily and non-invasively monitored during repeated-loading fatigue testing. Nonetheless, crack initiation has not been previously explored in algal specimens.

In this study, I address this gap in our understanding of fatigue failure in macroalgae, using two species of red macroalgae. With techniques that directly assess the entire process of fatigue, from crack formation to crack growth to final failure, I examine biologically and mechanically relevant aspects of fatigue. In particular, I answer the following questions.

(1) Do macroalgal specimens, without cracks introduced, fail predictably by fatigue?

(2) What are the relative contributions of crack initiation and subsequent crack growth to failure by fatigue?

(3) Do biological characteristics of macroalgal fronds (species, life history phase, frond size, epiphytization and seasonal changes) affect crack initiation and fatigue failure? Do pull-to-break strengths display similar correlations with biological characteristics?

(4) How do frequency of loading and time-dependent damage processes affect fatigue failure?

(5) Over what time scales and for what frond sizes is fatigue failure relevant in the field?

MATERIALS AND METHODS

Collection and preparation

Mazzaella is a red alga (phylum Rhodophyta) with a flat-bladed morphology that grows both intertidally and subtidally. Its material properties are determined in large part by its cell wall composition, which includes fiber-forming polysaccharides such as cellulose and matrix polysaccharides such as sulfated galactans (e.g. Kloareg and Quatrano, 1988; Craigie, 1990; Chopin et al., 1999). *Mazzaella* was selected for experimentation because it had previously proven amenable to repeated-loading testing (Mach et al., 2007b), and its flat-bladed morphology facilitated test-specimen preparation as well as photographic documentation of crack formation during fatigue testing.

Mazzaella flaccida (Setchell and Gardner) Fredericq was gathered from intertidal rocks at Hopkins Marine Station (HMS), Pacific Grove, CA, USA. Pull-to-break and fatigue tests of *M. flaccida* were conducted at HMS. *Mazzaella splendens* (Setchell and Gardner) Fredericq was collected from the floating dock at Friday Harbor Laboratories (FHL) on San Juan Island, WA, USA. Pull-to-break and fatigue tests of *M. splendens* were conducted at FHL.

At both testing locations, specimens were stored after collection in running-seawater aquaria, and testing occurred within 5 days. Before testing, the length and reproductive status of each frond were documented, with blades cross-sectioned and observed under a compound microscope to confirm reproductive status of tetrasporophyte, female gametophyte and male gametophyte fronds. Only fronds with reproductive structures in some portion of the blade were used for experiments. For *M. flaccida*, frond lengths ranged from 9 to 31 cm, and for *M. splendens*, lengths ranged from 12 to 40 cm.

For all pull-to-break and fatigue testing, dumbbell-shaped test specimens (Fig. 1A) of rectangular cross-section were cut from the flat blades of *Mazzaella* fronds, with each specimen's long axis aligned with the blade's long axis (Fig. 1B). The top and bottom large portions of dumbbell specimens were gripped within the testing apparatus during experiments. At HMS, each specimen's middle portion was flanked top and bottom by curving portions of radius 1.9 cm. Each specimen was prepared by placing a machined, aluminium template onto a *Mazzaella* blade and then tracing the template with a sharp scalpel. Each specimen edge, excluding the large, gripped portions, was cut with one continuous motion of the scalpel to ensure smoothness of the edge. To facilitate gripping, 3.0 cm by 1.5 cm pieces of sandpaper (Norton® waterproof sandpaper, grit P220, weight B) were affixed with cyanoacrylate glue onto both sides of the two large regions of each test specimen, with the rough side of each sandpaper piece facing away from the seaweed. During testing, tensile forces were applied along the long axis of each specimen, in the same manner that *Mazzaella* blades are loaded in the field, and failure of specimens occurred in the narrow portions of specimens. In a few cases when failure occurred near the gripped regions of test specimens, the specimen and trial were eliminated from further analyses. The thickness of the narrow region varied with the life history phase of the algal frond being tested but was nearly constant throughout each individual specimen. This thickness, usually between 0.3 and 0.6 mm, was measured with calipers prior to testing of each specimen.

At FHL, dumbbell-shaped specimens of *M. splendens* were prepared similarly. Due to size limitations of the testing apparatus, specimens had smaller dimensions (Fig. 1).

Testing apparatuses

At HMS, pull-to-break and fatigue tests were executed with a hydraulically driven tensometer. Several scripts written in LabView

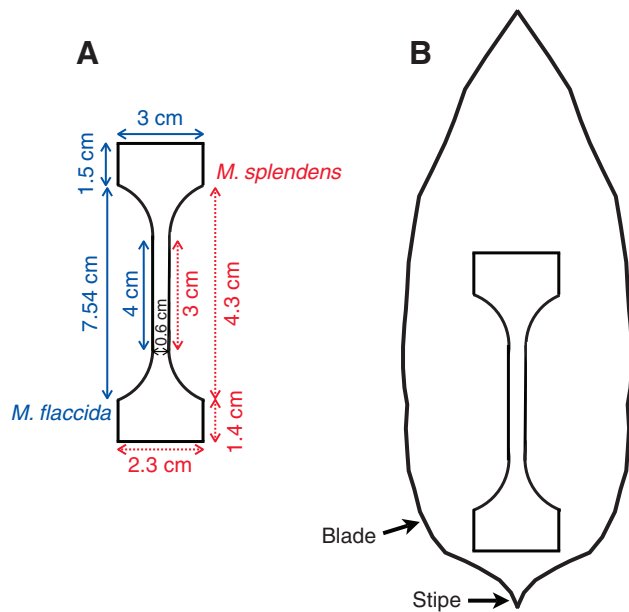


Fig. 1. (A) Diagram of specimens used in pull-to-break and fatigue tests. *Mazzaella flaccida*, tested at HMS, had larger dimensions than *M. splendens*, tested at FHL. The top and bottom larger portions of specimens were gripped within the testing apparatus. Fracture occurred within the narrow (0.6 cm wide) central portion of specimens. (B) Diagram of a *M. flaccida* frond indicating orientation of specimen cut from blade. The stem-like stipe is also depicted.

(National Instruments Corporation, Austin, TX, USA) controlled the position of the driving arm (Parker Electrohydraulics, Elyria, OH, USA; PLA series) through a 0–10 V signal from a 16-bit input/output board (National Instruments Corporation, model PCI-6221).

Force (N) on samples was measured with a cantilever-style force transducer (World Precision Instruments, Sarasota, FL, USA; FORT5000, 5000 g maximum load) paired with an amplifier (World Precision Instruments, Transbridge 4M), with a force measurement accuracy of 0.005 N. The transducer and its mount were waterproofed (Vishay® Micro-Measurements, Malvern, PA, USA; M-Coat J-1 Kit, polysulfide protective coating system). In analyses of failure, engineering stress (Pa) was computed as applied force divided by unstressed specimen cross-sectional area at the point of failure.

Extension of test specimens was determined from the position controller of the hydraulic arm, given negligible deflection of the force transducer beam, and engineering strain was calculated as change in specimen length divided by initial length. Engineering strain determined in this way does not account for variation in strain throughout dumbbell-shaped specimens (e.g. Bowman et al., 1998). However, measuring the strain of entire specimens avoids alteration of material properties by more intrusive and less accurate local strain measurement techniques, which would be particularly disruptive for the thin, highly extensible macroalgal blades used here. Engineering strains in this study should not be interpreted as exact values for materials examined; nonetheless, they allow comparison across tests for the same specimen type.

The top and bottom 3 cm by 1.5 cm portions of the dumbbell-shaped specimens, with sandpaper pieces attached, were gripped between stainless-steel and aluminium strips lined with rubber and tightened together with screws prior to loading. During testing, the

rubber lining, 1.3 mm thick, deformed slightly, but a prior analysis of this deformation (Mach et al., 2007b) showed it to have negligible effect on measurements of specimen extension.

During repeated-loading fatigue testing, crack formation in specimens was monitored through photographs taken by a computer-controlled digital camera (Canon, Lake Success, NY, USA; EOS 30D). All samples were bathed during testing in chilled, filtered seawater maintained at 12–13°C, typical surface seawater temperatures in Pacific Grove.

At FHL, pull-to-break and fatigue tests were performed with an Instron® high-stiffness load frame (Instron, Norwood, MA, USA; Series 5500, Model 5565). Instron® Merlin™ software was used to control the load frame's moving crosshead.

Force on each specimen was measured with a 50 N Load Cell (Instron, Type 2525-817), and in analyses of failure, engineering stress in specimens was calculated as for specimens at HMS. Specimen extension was determined from the load-frame position controller, and engineering strain was calculated as for specimens at HMS.

Dumbbell-shaped specimens with attached sandpaper pieces were mounted in the testing apparatus as at HMS. During testing, specimens were not photographed at FHL but were bathed in chilled, filtered seawater also maintained at typical local sea-surface temperatures, 10–11°C.

Pull-to-break tests

At HMS, *M. flaccida* specimens were prepared as described above, from tetrasporophyte ($N=17$), female gametophyte ($N=17$) and male gametophyte ($N=17$) fronds, during August 2008. Test specimens all contained reproductive structures, tetrasporophytes with tetrasporangial sori, female gametophytes with cystocarps, and male gametophytes with spermatangial sori. At FHL, *M. splendens* specimens were prepared similarly, from tetrasporophyte ($N=31$) and female gametophyte ($N=31$) fronds, during September 2007. All fronds contained reproductive structures, but some test specimens did not: 22 tetrasporophyte test specimens contained tetrasporangial sori, while 9 did not; 25 female gametophyte test specimens contained cystocarps, while 6 did not. Specimens without reproductive structures were cut from fronds not completely covered with reproductive structures. At HMS and FHL, once mounted in the loading apparatus, specimens were stretched at a strain rate of 0.19 s^{-1} until breakage occurred. Maximum recorded force (N) was used to determine engineering breaking stress (Pa). Data were analyzed statistically using *t*-tests (Microsoft® Excel) and ANOVA analyses (JMP®, version 4.0.4, SAS Institute, Cary, NC, USA).

Fatigue tests

At HMS, repeated fatigue loadings were stress controlled and sinusoidal in profile. Once mounted in the loading apparatus, a specimen was extended repeatedly and continuously from 0 N to a maximum force selected for each specimen, ranging from 1 to 5.5 N. These loadings, always with a minimum force of 0 N, were biologically relevant: in the field, wave-induced water flows extend previously unstressed seaweeds in tension, with no mean stress maintained between loadings. Similarly, in experiments, loading force and thus engineering stress cycled between minimums of 0 N (or 0 Pa) and selected maximum values until each sample broke. The number of loading cycles before failure was determined as the number of times force oscillated from 0 N to maximum force and back to 0 N again.

Over the course of each fatigue trial, specimens elongated, with maximum engineering strain increasing even though maximum

imposed force and stress remained constant. Maximum strain achieved in each loading cycle was monitored and recorded through a LabView script.

Periodic photographs were taken at a rate corresponding to maximum loading force and thus fatigue trial duration: every 30 s for trials with a maximum force of 5.5 N and every 30 min for trials with a maximum force of 1 N, with intermediate photographic rates at intermediate loading forces. Photographs were analyzed in ImageJ (Research Services Branch, National Institute of Mental Health, Bethesda, MD, USA, version 1.37) to determine (1) the number of loading cycles to formation of the first visible fatigue crack in each sample and (2) the location of this first fatigue crack: on the specimen edge or not; for tetrasporophytes and female gametophytes, associated with reproductive structures or not; and in male gametophyte specimens with endophytes, associated with endophytes or not. Endophytes were assessed only in male gametophyte specimens because endophytes were readily visible in male gametophytes but not in female gametophytes and tetrasporophytes, in which cystocarps and tetrasporangial sori obscured endophytes.

Mazzaella flaccida specimens were tested from all three flat-bladed life history phases, tetrasporophyte, male gametophyte and female gametophyte, from October 2007 to July 2008. Cycling occurred primarily at 1 Hz ($N=129$: 43 tetrasporophytes, 44 male gametophytes, 42 female gametophytes), with the effects of loading at 0.5 Hz ($N=42$: 14 tetrasporophytes, 14 male gametophytes, 14 female gametophytes) and 2 Hz ($N=30$: 13 tetrasporophytes, 6 male gametophytes, 11 female gametophytes) assessed as well. In the field, *M. flaccida* experiences waves every 9–10 s, but in the resulting complex, wave-induced flows, substantial velocities occur over fractions of seconds to several seconds. Loading frequencies from 0.5 to 2 Hz thus span typical loading frequencies in the field, although wave-associated loadings are not continuous over time, imposed instead approximately every 10 s.

Further, to determine the effects of season, the 1 Hz *M. flaccida* tests were conducted throughout the year, during October to December 2007 ($N=95$: 31 tetrasporophytes, 33 male gametophytes, 31 female gametophytes), during April 2008 ($N=16$: 6 tetrasporophytes, 5 male gametophytes, 5 female gametophytes), and during July 2008 ($N=18$: 6 tetrasporophytes, 6 male gametophytes, 6 female gametophytes).

At FHL, fully stress-controlled, sinusoidal loading was not possible given the software available. Instead, for each sample, loading was of sawtooth waveform, with loading frame crosshead speed constant, set at the beginning of each trial to a value between 600 and 800 mm min⁻¹. The crosshead cycled at a constant rate between 0 N and a specified maximum force set for each sample, ranging from 1.3 to 8 N. As at HMS, a loading cycle was defined as one oscillation of force from 0 N to the specified maximum force and then back to 0 N. The crosshead speed was selected for each sample so that the combination of loading force range and crosshead speed would give repeated loading at approximately 0.5 Hz. Cycling was achieved at 0.40±0.10 Hz (mean ± s.d.; $N=86$). Samples were loaded continuously in this manner until breakage occurred. For samples that withstood more than 9000 cycles, loading was paused briefly with the specimen unstretched, for about 5 min approximately every 9000 cycles, to save data and then restart loading.

Mazzaella splendens specimens from tetrasporophyte fronds, with and without tetrasporangial sori ($N=46$: 28 with sori, 18 without sori), and from female gametophyte fronds, with and without cystocarps ($N=41$: 36 with cystocarps, 5 without cystocarps), were tested during August and September 2007.

Fatigue data analysis

For all specimens, fatigue failure was characterized with log–log plots of loading stress *versus* number of cycles to breakage. Engineering convention was followed for these fatigue plots, as usually done for biological materials, with the independent variable, loading stress, on the ordinate and the dependent variable, cycles to failure, on the abscissa (e.g. Hearle, 1967; Caler and Carter, 1989; Choi and Goldstein, 1992; Zioupos et al., 1996; Schechtman and Bader, 1997; Bowman et al., 1998; Wren et al., 2003). Linear regressions were fitted to these log–log plots of fatigue behavior. For *M. flaccida* (HMS) and *M. splendens* (FHL), the effects on fatigue behavior of factors such as life history phase, species and frond size were determined. For *M. flaccida* data only, the effects on fatigue behavior of season and loading frequency were also assessed. Data for specimens loaded at different frequencies indicated indirectly the effects on fatigue behavior of testing duration. Log–log fatigue behavior plots were evaluated with ANCOVA analyses (JMP®).

Additionally, timing and location of initial crack formation, along with strain changes over the course of loading, were analyzed for *M. flaccida*. To evaluate the timing of the formation of the first visible cracks during fatigue tests, a crack formation index, C , comparing the number of cycles to specimen breakage, N_{breakage} , with the number of cycles to formation of a visible crack, $N_{\text{crack formation}}$, was used for each specimen:

$$C = \frac{N_{\text{breakage}} - N_{\text{crack formation}}}{N_{\text{breakage}}} \quad (1)$$

In other words, a C value of 0 indicates a specimen forming a visible crack and breaking in the same loading cycle, whereas C values nearer to 1 indicate specimens forming visible cracks closer to the beginning of fatigue tests and then enduring many loading cycles before breakage.

Locations of crack formation were documented, as described in the previous section. Additionally, a crack-simulation procedure was used to determine whether cracks formed in specific locations (in or near endophytes or reproductive structures) more often than expected by chance alone. In photographs of specimens, crack formation was simulated by randomly placing ‘cracks’ on specimens and then determining the frequency of crack association with endophytes, cystocarps and tetrasporangial sori. These association frequencies were compared with values measured for fatigue specimens.

To complete this analysis, the average length and opening displacement (Fig. 2A) of first-photographed fatigue cracks were determined for female gametophyte, tetrasporophyte and male gametophyte specimens. Although first-photographed fatigue cracks were elliptical in specimen photographs because specimens were extended beyond resting length (Fig. 2A), simulated cracks were approximated as rectangular, of width equal to crack length and height equal to crack opening displacement. For 10 randomly selected specimens for each category (female gametophytes with cystocarps, tetrasporophytes with tetrasporangial sori, and male gametophytes with endophytes), 20 rectangular cracks of average first-detected dimensions for the life history phase were generated. Simulated cracks had the following dimensions: 0.48 mm width by 0.23 mm height for female gametophytes, 0.59 mm by 0.30 mm for tetrasporophytes, and 0.59 mm by 0.32 mm for male gametophytes. In photographs taken of specimens during testing, analyzed previously for crack formation timing and location, simulated cracks were placed at random coordinates within the narrow, rectangular, 0.6 cm by 4 cm portion of each specimen (Fig. 2B). It was then determined whether each simulated crack was associated

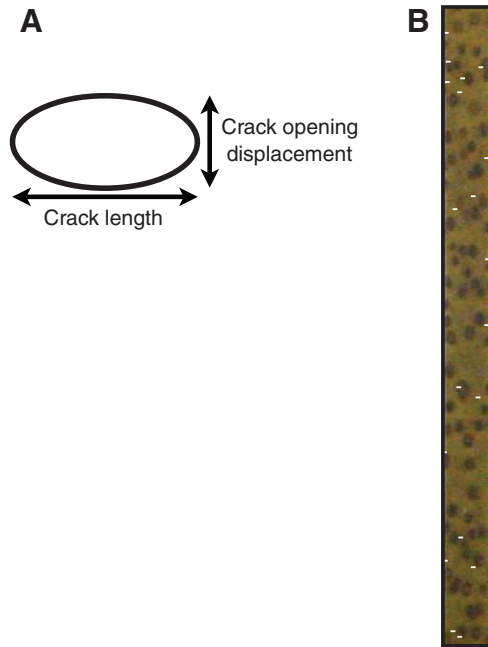


Fig. 2. Diagrams used in explanation of crack-simulation procedure. (A) Dimensions quantified for first-observed fatigue cracks. (B) The 0.6 cm by 4 cm region of a female gametophyte specimen with cystocarps, extended during testing; 20 white rectangular simulated cracks have been randomly placed over the test-specimen photograph.

with structures of interest (cystocarps in female gametophyte specimens, tetrasporangial sori in tetrasporophyte specimens, and endophytes in male gametophyte specimens). If located in the middle of or along the edge of a structure of interest, a simulated crack was scored as associated with that structure, as done for actual fatigue cracks in tested specimens. The cystocarp, tetrasporangial sorus and endophyte association frequencies measured in actual fatigue specimens were compared using Pearson's chi-square test to frequencies determined for simulated cracks.

Additionally, to further inform observations of crack locations, the surface area of the randomly selected, crack-simulation specimens that was covered with cystocarps in female gametophytes, with tetrasporangial sori in tetrasporophytes and with endophytes in male gametophyte specimens with endophytes was quantified. For female gametophyte and tetrasporophyte specimens, an area of approximately 0.4 cm^2 within the narrow portion of the specimen was haphazardly selected in the photograph of each extended specimen. In ImageJ, the percentage of this selected area covered with cystocarps or tetrasporangial sori was quantified. For male gametophyte specimens, the proportion of the entire narrow, 0.6 cm by 4 cm region of the specimen covered with endophytes was quantified in ImageJ.

To characterize changes in maximum strain during fatigue testing, two strain change indices quantified strain changes over the first 20 loading cycles of fatigue tests and over the entire course of fatigue tests:

$$S_{20} = \frac{\epsilon_{\max,20} - \epsilon_{\max,\text{initial}}}{\epsilon_{\max,\text{initial}}}, \quad (2)$$

$$S_{\text{entire}} = \frac{\epsilon_{\max,\text{final}} - \epsilon_{\max,\text{initial}}}{\epsilon_{\max,\text{initial}}}. \quad (3)$$

S_{20} , the strain change index for the first 20 loading cycles, is calculated from maximum strain in the 20th loading cycle, $\epsilon_{\max,20}$, and maximum strain in the first loading cycle, $\epsilon_{\max,\text{initial}}$. Strain changed most dramatically during the first loading cycles of fatigue experiments; strain change after 20 cycles was arbitrarily chosen to represent this initial, rapid change in strain. S_{entire} , the strain change index for entire fatigue tests, is determined from maximum strain at the end of the fatigue test, $\epsilon_{\max,\text{final}}$, and $\epsilon_{\max,\text{initial}}$.

Drag coefficients

To determine fatigue experienced by *M. flaccida* in the field, drag on *M. flaccida* was measured over a range of water velocities, from 0.3 to 9.5 m s^{-1} , in the laboratory. When exposed to water movement, *M. flaccida* fronds reorient almost completely in the direction of flow (e.g. Denny and Gaylord, 2002), experiencing wave-induced forces in tension across their blades. Drag (N) has been established as the primary force acting on seaweeds exposed to breaking waves (Gaylord et al., 1994; Gaylord, 2000; Boller and Carrington, 2006a). At high velocities characteristic of wave-swept shores, drag force, F_D , can be modeled as:

$$F_D = \frac{1}{2} \rho A C_D u^2, \quad (4)$$

where ρ is fluid density; A is a representative area, here of an algal frond; C_D is a dimensionless drag coefficient, which varies with frond shape and with frond reconfiguration that occurs as water velocity increases (e.g. Vogel, 1984; Carrington, 1990; Boller and Carrington, 2006b); and u is water velocity. In this study, ρ was taken as the density of freshwater in flume experiments and as seawater density for subsequent field calculations, representative area A was taken as the single-sided surface area of a frond pressed flat, as conventionally done for macroalgae (Carrington, 1990; Denny and Gaylord, 2002), and C_D was determined from flume experiments.

Mazzaella flaccida fronds were tested in a recirculating flume at eight water velocities ranging from 0.3 to 3.8 m s^{-1} and in a gravity flume at three velocities spanning 5.4 to 9.5 m s^{-1} . Representative area A was measured prior to testing by gently flattening each frond against a white background using small brass weights painted black. A photograph of each flattened frond and an adjacent scale bar was taken and analyzed in ImageJ to determine single-sided surface area of the flattened frond, which was used for A .

The recirculating flume was similar to the flume described previously in detail by Boller and Carrington (Boller and Carrington, 2006b). Its force transducer (Bokam Engineering, Santa Ana, CA, USA; US-06002, a multi-axial transducer used for electronic 'joystick' controls), with four instrumentation amplifiers (Analog Devices, Norwood, MA, USA; AD627), measured force in the x - and y -directions perpendicular to its main axis, with data recorded to file through a LabView script. The high velocity gravity flume and associated force transducer have been described previously by Miller and Gaylord (Miller and Gaylord, 2007). Again, data were recorded to file through a LabView script.

During testing in both flumes, the base of each frond's stipe was inserted with cyanoacrylate glue into aluminium rods attached to the force transducers. The aluminium rods did not protrude into the flumes, instead remaining flush with the flume's wall surfaces, and drag on aluminium rods alone was found to be negligible. Each frond was exposed to a range of velocities in one of the flumes, with drag force at each velocity measured with the force transducer. From frond area A and measured drag force F_D , drag coefficient C_D was determined for each velocity u .

To relate laboratory fatigue results to flow environments in the field, measured drag coefficients were used to calculate wave-

imposed velocities corresponding to stresses applied to *M. flaccida* in the laboratory. Force application varied between fatigue testing and exposure to flow, with force applied uniformly to a specimen during fatigue testing and with force graded over the length of a frond in flume or field flows. Comparison between the two force-application modes considered the stresses experienced uniformly over the narrow portions of fatigue-tested specimens and the maximal stresses due to drag, experienced in the bases of blades, above the stipes, for fronds exposed to flow.

For representative big, medium and small fronds, maximum stress imposed in the laboratory was thus converted to equivalent drag force using representative frond dimensions for blade bases. Drag force was then translated into wave-imposed water velocity by solving Eqn 4 for u and using measured values for C_D and representative frond areas A . Loading cycles to breakage, as a function of wave-imposed water velocity, were determined for each life history phase and frond size from fatigue results for the *M. flaccida* life history phases and correction coefficients necessitated by log-log transformations (Beauchamp and Olson, 1973; Baskerville, 1972; Sprugel, 1983).

RESULTS

Pull-to-break tests

Mazzaella flaccida specimens had an average strength \pm s.d. of 2.41 ± 0.78 MPa. More specifically, male gametophyte specimens possessed a strength of 3.18 ± 0.51 MPa, followed by tetrasporophyte specimens (2.16 ± 0.39 MPa) and then by female gametophyte specimens (1.88 ± 0.70 MPa). The ordinate of Fig. 3A depicts, on a logarithmic scale, these pull-to-break strengths of *M. flaccida* specimens. Life history phase had a significant effect on pull-to-break strength, with male gametophyte specimens significantly stronger than female gametophytes and tetrasporophytes, which were statistically indistinguishable (ANOVA, $F_{2,48}=26.78$, $P \leq 0.001$; variances homogeneous: Brown-Forsythe test, $P=0.34$; Tukey HSD).

Mazzaella splendens specimens had an average strength of 3.14 ± 0.90 MPa. Tetrasporophyte specimens (3.48 ± 0.74 MPa) were stronger than female gametophyte specimens (2.79 ± 0.93 MPa; two-tail t -test, equal variances, $t=3.22$, $P < 0.01$). The ordinate of Fig. 3B depicts these data for *M. splendens* tetrasporophytes and female gametophytes. The strength of tetrasporophyte specimens without tetrasporangial sori, 4.12 ± 0.64 MPa, exceeded the strength of specimens with tetrasporangial sori, 3.22 ± 0.62 MPa (two-tail t -test, equal variances, $t=3.66$, $P=0.001$). Likewise, the strength of female gametophytes without cystocarps, 3.88 ± 1.01 MPa, exceeded the strength of specimens with cystocarps, 2.53 ± 0.71 MPa (two-tail t -test, equal variances, $t=3.84$, $P < 0.001$).

A comparison of *M. flaccida* and *M. splendens* tetrasporophytes and female gametophytes indicated that the strength of *M. splendens* for these two life history phases, 3.14 ± 0.90 MPa, exceeded that of *M. flaccida* for the two life history phases, 2.02 ± 0.57 MPa (two-tail t -test, unequal variances, $t=7.41$, $P \leq 0.001$). The ordinate of Fig. 4 shows these average strengths for the two species.

Fatigue tests

Life history phases

Fatigue data for *M. flaccida* loaded at 1 Hz, collected throughout the year, are shown by life history phase in Fig. 3A. These data for $\log N_{\text{breakage}}$ versus $\log \sigma_{\text{max}}$, where N_{breakage} is number of cycles to specimen breakage and σ_{max} is maximum stress imposed in each loading cycle, were fitted with regression equations given in Table 1. Linear regressions for the three life history phases had

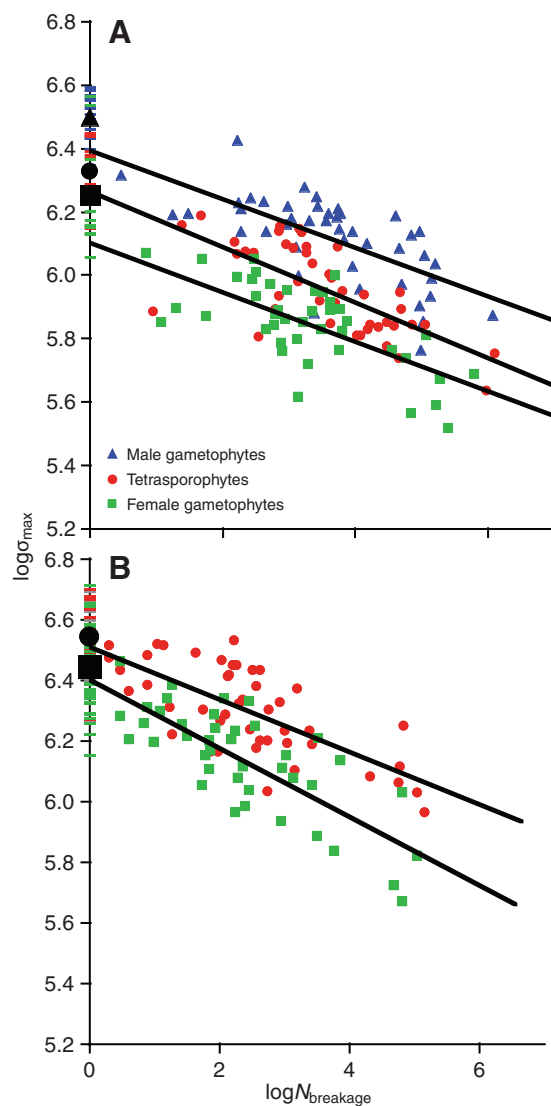


Fig. 3. Fatigue data for (A) *M. flaccida* and (B) *M. splendens*, shown on logarithmic axes as number of loading cycles to breakage, N_{breakage} , versus maximum loading stress per cycle, σ_{max} (Pa). Additionally, pull-to-break strengths (Pa) are given on the ordinate, also on a logarithmic scale. *M. flaccida* fatigue data in A include 1 Hz fatigue tests only. For fatigue data in A and B, blue triangles represent male gametophyte test specimens; red circles, tetrasporophyte specimens; and green squares, female gametophyte specimens. Pull-to-break data are given as dashes on the ordinate, blue for male gametophyte specimens, red for tetrasporophyte specimens, and green for female gametophyte specimens. Average pull-to-break strength is shown as a black triangle for male gametophytes, a black circle for tetrasporophytes, and a black square for female gametophytes. Regression lines are shown, and equations for regressions are given in Table 1.

indistinguishable slopes and demonstrated a significant effect of life history phase (ANCOVA: life history phase \times $\log N_{\text{breakage}}$, $F_{2,123}=0.18$, $P=0.83$; life history phase, $F_{2,123}=93.05$, $P \leq 0.001$). Male gametophytes were stronger in fatigue than tetrasporophytes, which were stronger than female gametophytes (Tukey HSD).

Fatigue data for *M. splendens* are given by life history phase in Fig. 3B. These data were also fitted with regression equations, given in Table 1. Linear regressions for the two life history phases had indistinguishable slopes and showed a significant effect of life

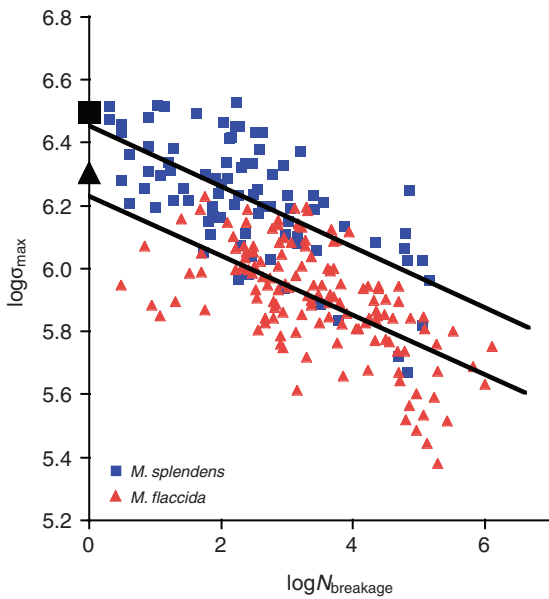


Fig. 4. Fatigue data for *M. splendens* (blue squares) and *M. flaccida* (red triangles). On logarithmic axes, the plot depicts number of loading cycles to breakage, N_{breakage} , versus maximum loading stress per cycle, σ_{max} (Pa). *M. flaccida* data include fatigue tests at 0.5, 1 and 2 Hz. For each species, data for only tetrasporophyte and female gametophyte specimens are given; male gametophyte data collected for *M. flaccida* have been excluded from the plot. Regression lines are shown, with regression equations described in Table 1. Average pull-to-break strengths for each species (male gametophytes excluded) are given on the ordinate, with a black square for *M. splendens* and a black triangle for *M. flaccida*.

history phase, with tetrasporophytes stronger in fatigue than female gametophytes (ANCOVA: life history phase \times $\log N_{\text{breakage}}$, $F_{1,83}=1.78$, $P=0.19$; life history phase, $F_{1,83}=52.05$, $P\leq 0.001$).

Species

Fatigue data for *M. splendens* and *M. flaccida* female gametophytes and tetrasporophytes are shown by species in Fig. 4. For *M. flaccida*, all fatigue data for these two life history phases, including 0.5, 1 and 2 Hz loadings, are depicted. Linear regressions for the two species (Table 1) had indistinguishable slopes and displayed a significant effect of species, with *M. splendens* stronger in fatigue than *M. flaccida* (ANCOVA: species \times $\log N_{\text{breakage}}$, $F_{1,220}=0.02$, $P=0.89$; species, $F_{1,220}=108.91$, $P\leq 0.001$).

Seasons

Mazzaella flaccida 1 Hz fatigue data are given by season of testing (October through to December, April and July) in Fig. 5. Linear regressions for these data had indistinguishable slopes and revealed no effect of season (ANCOVA: season \times $\log N_{\text{breakage}}$, $F_{2,123}=0.73$, $P=0.48$; season, $F_{2,123}=0.88$, $P=0.42$).

Loading frequency

Mazzaella flaccida data for all life history phases are depicted by loading frequency in Fig. 6. Linear regressions for these data had indistinguishable slopes and displayed a marginal effect of loading frequency (ANCOVA: frequency \times $\log N_{\text{breakage}}$, $F_{2,195}=2.84$, $P=0.06$; frequency, $F_{2,195}=3.40$, $P=0.04$). *Mazzaella flaccida* loaded at 2 Hz was slightly stronger than *M. flaccida* loaded at 1 and 0.5 Hz, for which there was no significant statistical difference (Tukey

Table 1. Linear regressions for *M. flaccida* and *M. splendens* fatigue data in Figs 3 and 4

Figure	Data category	<i>m</i>	<i>b</i>	<i>R</i> ²
3A	Male gametophyte, 1 Hz	-0.077	6.394	0.46
3A	Tetrasporophyte, 1 Hz	-0.087	6.264	0.48
3A	Female gametophyte, 1 Hz	-0.078	6.102	0.46
(3A)	All <i>M. flaccida</i> , 1 Hz	-0.068	6.212	0.20
3B	Tetrasporophyte	-0.087	6.511	0.50
3B	Female gametophyte	-0.113	6.402	0.60
4	<i>M. splendens</i>	-0.097	6.454	0.42
4	<i>M. flaccida</i> , no males	-0.094	6.230	0.38

Regression equation: $\log \sigma_{\text{max}} = m \log N_{\text{breakage}} + b$, where σ_{max} is maximum stress per cycle, N_{breakage} is number of cycles to breakage, *m* and *b* are fitted constants. All regressions are highly significant ($P \leq 0.001$).

HSD). The overall similarity in fatigue behavior at different loading frequencies provides indirect evidence that specimen degradation due to testing duration did not greatly affect measured fatigue properties.

Fatigue cracks: timing and location of formation

I excluded from analyses of crack-formation timing five *M. flaccida* specimens for which crack-formation photography was interrupted. For the remaining *M. flaccida* specimens, the crack formation index *C*, indicating the relative timing of first-visible crack formation in fatigue experiments, was calculated as 0.120 ± 0.061 for male gametophytes (mean \pm 95% confidence interval; $N=61$), 0.207 ± 0.058 ($N=68$) for tetrasporophytes, and 0.222 ± 0.061 ($N=67$) for female gametophytes (Fig. 7). *C* differed with life history phase (ANOVA on square-root-transformed data, $F_{2,196}=5.03$, $P < 0.01$; variances

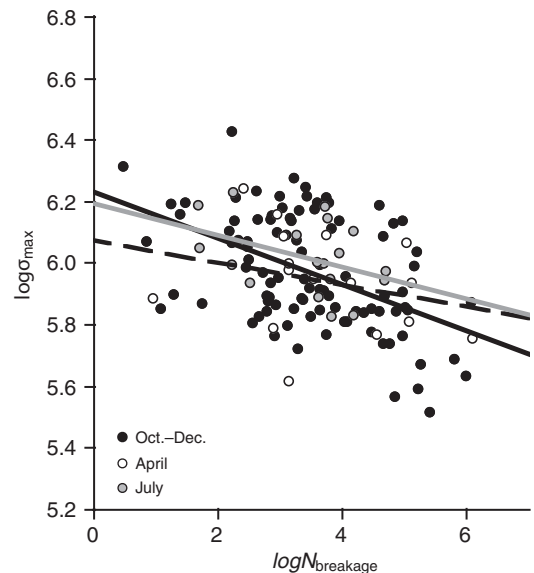


Fig. 5. Fatigue data for *M. flaccida* tested at 1 Hz, given by season of testing. Data include 1 Hz fatigue tests for all three life history phases. On logarithmic axes, the plot shows number of loading cycles to breakage, N_{breakage} , versus maximum loading stress per cycle, σ_{max} (Pa). Black circles represent fatigue tests from October to December 2007; white circles, from April 2008; and gray circles, from July 2008. Linear regression equations are as follows: for October to December (black line), $\log \sigma_{\text{max}} = -0.075 \log N_{\text{breakage}} + 6.232$, $R^2 = 0.23$; for April (dashed line), $\log \sigma_{\text{max}} = -0.036 \log N_{\text{breakage}} + 6.071$, $R^2 = 0.07$; and for July (gray line), $\log \sigma_{\text{max}} = -0.052 \log N_{\text{breakage}} + 6.196$, $R^2 = 0.17$.

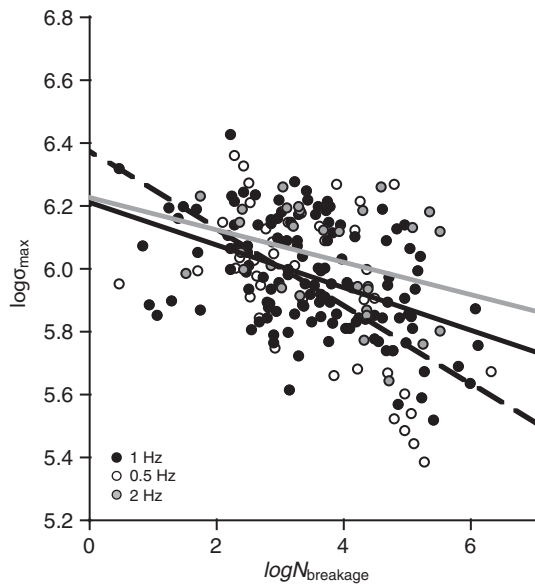


Fig. 6. Fatigue data for *M. flaccida*, shown by loading frequency. The plot includes all data for the three tested life history phases. On logarithmic axes, the plot shows number of loading cycles to breakage, N_{breakage} , versus maximum loading stress per cycle, σ_{max} (Pa). Black circles indicate fatigue tests at 1 Hz; white circles, 0.5 Hz; and gray circles, 2 Hz. Linear regression equations are as follows: for 1 Hz (black line), $\log \sigma_{\text{max}} = -0.068 \log N_{\text{breakage}} + 6.212$, $R^2 = 0.20$; for 0.5 Hz (dashed line), $\log \sigma_{\text{max}} = -0.124 \log N_{\text{breakage}} + 6.376$, $R^2 = 0.33$; and for 2 Hz (gray line), $\log \sigma_{\text{max}} = -0.052 \log N_{\text{breakage}} + 6.226$, $R^2 = 0.12$.

homogeneous: Brown–Forsythe test, $P = 0.11$). Cracks formed later (and thus C was smaller) in male gametophyte specimens than in tetrasporophyte and female gametophyte specimens, for which crack timing did not differ (Tukey HSD).

Initial crack formation demonstrated the following associations with specimen edges, reproductive structures and endophytes. Of 140 initial cracks observed in specimens of all life history stages, 25 (17.9%) formed on specimens' lateral edges. Of 54 initial cracks

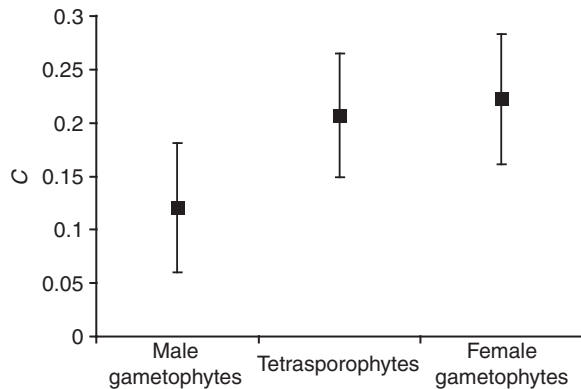


Fig. 7. Crack formation index, C , for *M. flaccida* male gametophytes, tetrasporophytes and female gametophytes, with 0.5, 1 and 2 Hz fatigue tests included in calculations. C is the difference between number of cycles to breakage, N_{breakage} , and number of cycles to crack formation, N_{crack} formation, with this difference normalized by N_{breakage} . Plot depicts mean $C \pm 95\%$ confidence interval for each life history phase.

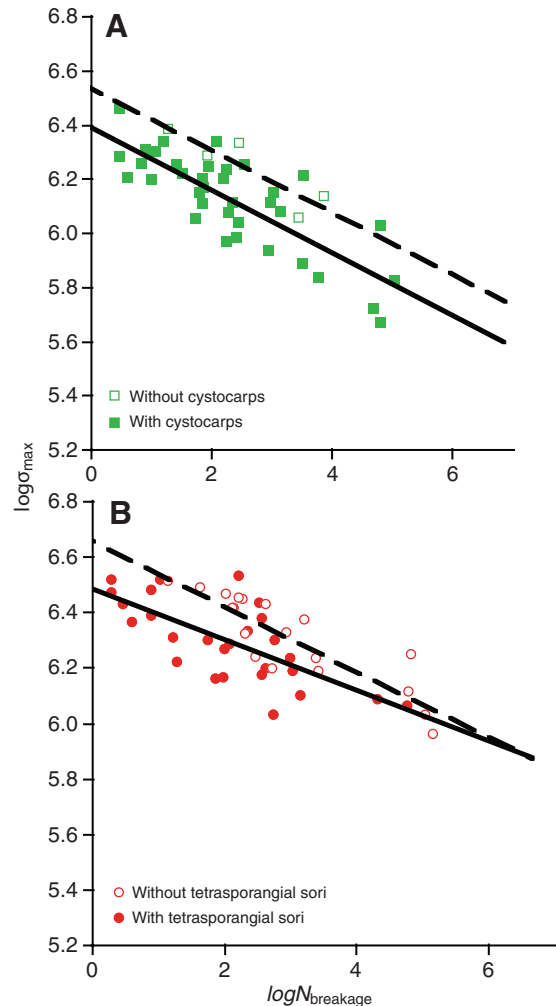


Fig. 8. Fatigue data for *M. splendens* female gametophytes (A) and tetrasporophytes (B), showing test specimens with (filled symbols) and without (open symbols) reproductive structures. On logarithmic axes, the plots depict number of loading cycles to breakage, N_{breakage} , versus maximum loading stress per cycle, σ_{max} (Pa). Linear regressions with the following equations are shown: for female gametophytes with cystocarps (solid line in A), $\log(\sigma_{\text{max}}) = -0.116 \log N_{\text{breakage}} + 6.391$, $R^2 = 0.65$; for female gametophytes without cystocarps (dashed line in A), $\log \sigma_{\text{max}} = -0.115 \log N_{\text{breakage}} + 6.536$, $R^2 = 0.78$; for tetrasporophytes with tetrasporangial sori (solid line in B), $\log \sigma_{\text{max}} = -0.092 \log N_{\text{breakage}} + 6.486$, $R^2 = 0.49$; for tetrasporophytes without tetrasporangial sori (dashed line in B), $\log \sigma_{\text{max}} = -0.118 \log N_{\text{breakage}} + 6.657$, $R^2 = 0.77$.

observed in female gametophyte specimens, 38 (70.4%) formed in the middle or along edges of cystocarps. Of 47 initial cracks observed in tetrasporophyte specimens, 35 (74.5%) formed in the middle or along edges of tetrasporangial sori. Of 39 initial cracks observed in male gametophytes, 6 (15.4%) formed in the middle or along edges of endophytes. Considering only the 13 male gametophyte specimens with endophytes in the narrow specimen breakage regions, I found that initial cracks were associated with endophytes in 46.2% (6 of 13) of these specimens.

Simulated, randomly located cracks had the following distributions. In cystocarpic specimens, 35.5% of simulated cracks (71 of 200, with 20 simulated cracks in each of 10 specimens) were associated with cystocarps, located in the middle or along the edges of cystocarps. In tetrasporangial specimens, 66% of simulated cracks

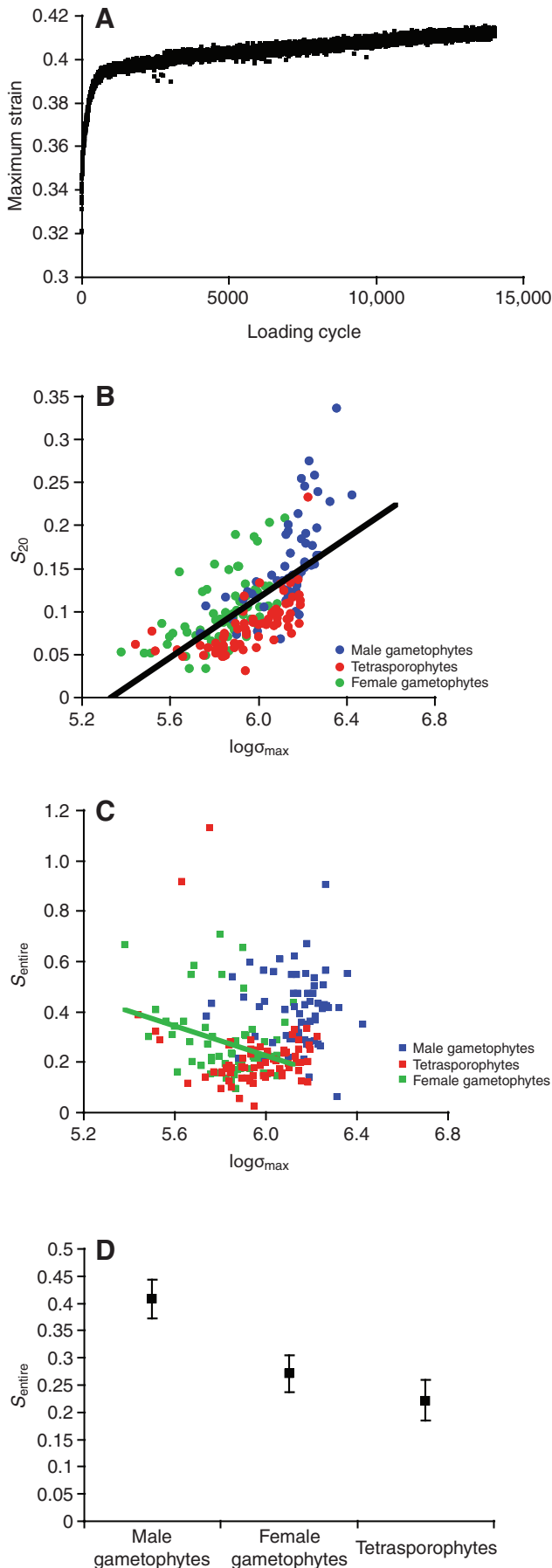


Fig. 9. (A) A representative plot of change in maximum strain during a fatigue test in which an *M. flaccida* specimen was loaded repeatedly to constant maximum stress. (B) Strain change index S_{20} , indicating change in maximum strain over the first 20 cycles of loading, as a function of maximum stress per cycle, σ_{\max} , applied to specimens. The abscissa is logarithmic. Plot shows data for all *M. flaccida* tested, with male gametophyte specimens represented by blue circles, tetrasporophyte specimens by red circles and female gametophyte specimens by green circles. Linear regression shown fits data for all three life history phases: $S_{20}=0.174\log\sigma_{\max}-0.930$, $R^2=0.44$, $P\leq 0.001$. (C) Strain change index S_{entire} , indicating change in maximum strain over entire fatigue tests, as a function of maximum stress per cycle, σ_{\max} (log scale). Again, data for all *M. flaccida* fatigue tests are depicted, with male gametophytes represented by blue squares, tetrasporophytes by red squares and female gametophytes by green squares. Linear regression fits data for female gametophytes: $S_{\text{entire}}=-0.291\log\sigma_{\max}+1.972$, $R^2=0.11$, $P=0.01$. (D) Mean strain change index $S_{\text{entire}} \pm 95\%$ confidence interval for *M. flaccida* male gametophytes, female gametophytes and tetrasporophytes. S_{entire} for male gametophytes was significantly greater than S_{entire} for female gametophytes and tetrasporophytes.

(132 of 200) were associated with tetrasporangial sori, located in the middle or along the edges of tetrasporangial sori. In male gametophyte specimens with endophytes, 3.5% of simulated cracks (7 of 200) were associated with endophytes, located in the middle or along the edges of endophytes.

A comparison of actual and simulated fatigue cracks indicated that actual cracks in female gametophytes were more frequently associated with cystocarps than would be expected for randomly forming cracks (Pearson's chi-square test, $P\leq 0.001$). Actual cracks in male gametophyte specimens with endophytes were also significantly more associated with endophytes than would be expected for randomly forming cracks (Pearson's chi-square test, $P\leq 0.001$). Actual cracks in tetrasporophyte specimens with tetrasporangial sori were no more associated with tetrasporangial sori than would be expected for randomly forming cracks (Pearson's chi-square test, $P=0.22$).

For the randomly selected specimens used for crack simulations, the proportions of specimens' flattened surface covered by cystocarps, tetrasporangial sori and endophytes were as follows: for female gametophytes, cystocarps covered $16.8\pm 5.2\%$ (mean \pm s.d.; $N=10$) of specimens; for tetrasporophytes, tetrasporangial sori covered $20.5\pm 7.8\%$ ($N=10$) of specimens; and for male gametophyte specimens with endophytes, endophytes covered $0.89\pm 0.81\%$ ($N=10$) of specimens.

The effects of reproductive structures were indirectly assessed with log-log fatigue plots of maximum loading stress versus number of cycles to breakage for *M. splendens* specimens with and without reproductive structures (Fig. 8). For female gametophyte specimens with and without cystocarps, linear regressions had similar slopes and demonstrated an effect of reproductive structures, with specimens without cystocarps stronger in fatigue than specimens with cystocarps (Fig. 8A; ANCOVA: structures \times $\log N_{\text{breakage}}$, $F_{1,37}=0.001$, $P=0.98$; structures, $F_{1,37}=8.14$, $P<0.01$). Likewise, for tetrasporophyte specimens with and without sori, linear regressions fitted to fatigue data had similar slopes and displayed an effect of reproductive structures (ANCOVA: structures \times $\log N_{\text{breakage}}$, $F_{1,42}=1.01$, $P=0.32$; structures, $F_{1,42}=11.19$, $P<0.01$). Specimens without tetrasporangial sori were stronger in fatigue than specimens with tetrasporangial sori (Fig. 8B).

Time-dependent changes

Maximum stress imposed cyclically during fatigue tests was constant for each specimen, but corresponding maximum cyclic strain

increased over the course of each run (e.g. Fig. 9A). For *M. flaccida*, change in maximum strain for the first 20 loading cycles, S_{20} , was correlated with maximum stress, σ_{\max} , imposed on specimens (Fig. 9B). However, change in maximum strain over entire fatigue tests, S_{entire} , showed little correlation with maximum stress (Fig. 9C). Of regression lines fitted to S_{entire} versus $\log\sigma_{\max}$ data for female gametophytes, male gametophytes, tetrasporophytes and all life history phases combined (Fig. 9C), only the regression line fitted to female gametophyte data had significant slope. Given there was little correlation between S_{entire} and maximum stress applied, I calculated average S_{entire} for each life history phase (Fig. 9D). For male gametophytes, S_{entire} was 0.41 ± 0.14 (mean \pm s.d.); for female gametophytes, S_{entire} was 0.27 ± 0.14 ; and for tetrasporophytes, S_{entire} was 0.22 ± 0.16 . Life history phase significantly affected S_{entire} , with S_{entire} significantly greater for male gametophytes than for female gametophytes and tetrasporophytes (ANOVA, $F_{2,195}=28.69$, $P\leq 0.001$; variances homogeneous: Brown–Forsythe test, $P=0.32$; Tukey HSD).

Size effects

For all 1 Hz *M. flaccida* data (Fig. 10A) and all *M. splendens* data (Fig. 10B), I determined whether blade length was correlated with strength in fatigue. For each specimen, I plotted length of the frond from which the specimen was taken, L_{frond} , versus residual r , where $r = \log N_{\text{breakage}} - \log N_{\text{breakage, predicted}}$. N_{breakage} is the measured number of loading cycles to breakage for each sample, and $N_{\text{breakage, predicted}}$ is the number of loading cycles to breakage predicted for each sample from regression equations given in Table 1. When positive, r indicates a given specimen withstood more loading cycles than predicted from its regression line (Table 1) – that is, at a given loading stress, the specimen endured more cycles before breaking than did typical fronds of that species and life history stage. When negative, r indicates a specimen broke sooner than expected on the basis of measured regression lines (Table 1). Frond length L_{frond} showed little correlation with residual r . Regression lines were fitted to data for each life history phase for each species, but only the regression line for *M. splendens* female gametophytes was marginally significant ($r=0.01L_{\text{frond}}-0.21$, $R^2=0.005$, $P=0.05$). However, this regression explains such a small fraction of the variance that it is biologically uninformative.

Laboratory-field comparisons

Measured drag coefficients for *M. flaccida* (Fig. 11) were fitted with the following curve: $C_D=0.0793u^{-0.7565}$, $R^2=0.8721$, where water velocity u has units of m s^{-1} and drag coefficient C_D is dimensionless.

To relate maximum stresses imposed during fatigue testing to wave-induced water velocities in the field, I used the above equation for C_D ; fatigue regressions for *M. flaccida* female gametophytes, tetrasporophytes and male gametophytes (Table 1); and representative dimensions for *M. flaccida* fronds. For blade thickness, I used average thicknesses determined for specimens during fatigue tests: 0.553 mm for female gametophytes ($N=67$), 0.466 mm for tetrasporophytes ($N=70$) and 0.376 mm for male gametophytes ($N=62$). For frond surface areas A and blade widths near frond bases, I selected representative plant dimensions from specimens used for drag coefficient determination: for a big frond, A was 0.0311 m^2 and width was 0.0586 m; for a medium frond, A was 0.0109 m^2 and width was 0.0440 m; and for a small frond, A was 0.0031 m^2 and width was 0.0221 m.

Fig. 12 depicts loading cycles to breakage, as a function of wave-imposed water velocity, for each life history phase and representative frond size. For a given water velocity, bigger fronds require fewer

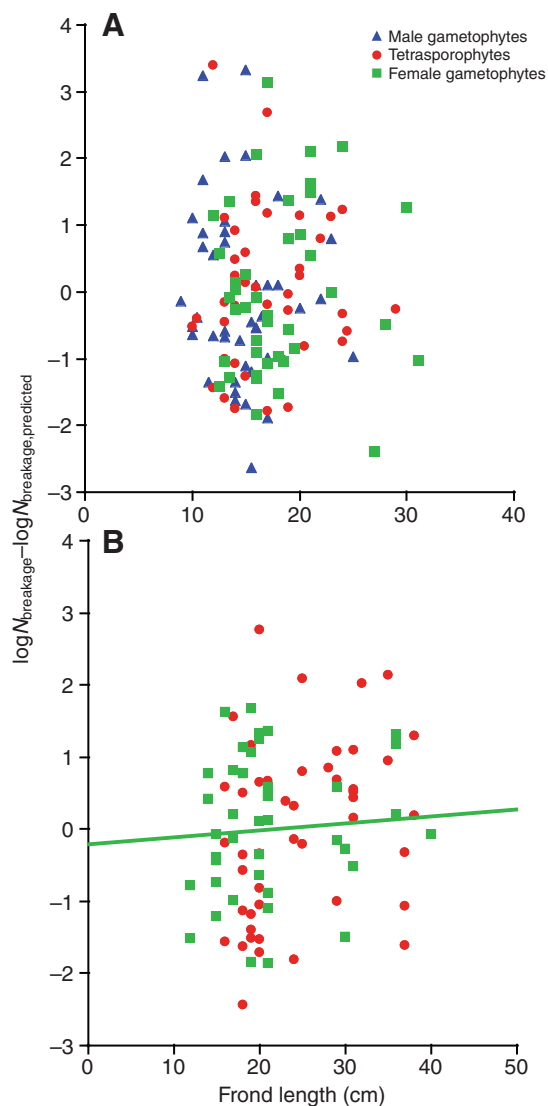


Fig. 10. Frond length versus $\log N_{\text{breakage}} - \log N_{\text{breakage, predicted}}$ for all 1 Hz *M. flaccida* data (A) and all *M. splendens* data (B), where N_{breakage} is the number of loading cycles to breakage and $N_{\text{breakage, predicted}}$ is the number of loading cycles predicted from regressions in Table 1. Blue triangles represent data from male gametophytes; red circles, tetrasporophytes; and green squares, female gametophytes. For life history phases tested for both species, only the linear regression for *M. splendens* female gametophytes, shown in B, was significant.

cycles for breakage. For a given frond size and water velocity, male gametophyte fronds survive longer than tetrasporophyte fronds, which in turn outlast female gametophyte fronds.

Results summary

A brief summation of the above findings may be helpful for subsequent discussion.

First and most fundamentally, these results demonstrate that the entire process of fatigue, including crack initiation, fatigue crack growth, and eventual specimen fracture, occurs predictably in the red, flat-bladed macroalga *Mazzaella*. The number of repeated loading cycles to failure decreased with increasing maximum loading stress repeatedly applied to specimens.

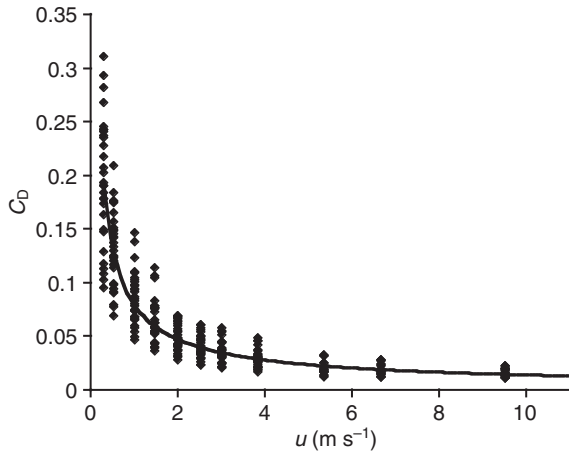


Fig. 11. Drag coefficient, C_D , as a function of water velocity, u (m s^{-1}), for *M. flaccida*. Drag data depicted were from two flumes: at eight velocities below 4 m s^{-1} , 30 data points were collected using a recirculating flume, and at three velocities from 5.4 to 9.5 m s^{-1} , 18 data points were collected using a high velocity, gravity flume. Curve equation is $C_D = 0.0793u^{-0.7565}$, $R^2 = 0.8721$.

Second, a number of influences on fatigue were elucidated. Fatigue behavior varied with life history phase for reproductive fronds, with male gametophytes stronger than tetrasporophytes, which were stronger than female gametophytes. Additionally, *M. splendens* was stronger in fatigue than *M. flaccida*. Fatigue behavior did not vary through the year or with frond size, and loading frequencies examined only marginally influenced fatigue behavior. Additionally, specimens displayed creep over the course of fatigue testing, progressively increasing in length.

Third, crack formation was assessed. Cracks commonly formed in association with reproductive structures in female gametophyte specimens and with endophytes, as observed in male gametophyte specimens. In general, crack initiation occurred fairly late in fatigue tests, with cracks often appearing after 80–90% of cycles required for breakage had passed and with fatigue failure soon resulting once cracks formed. The timing of crack initiation also differed across life history phases: cracks formed later in male gametophyte specimens than in tetrasporophyte and female gametophyte specimens.

Finally, comparisons of measured fatigue behaviors and field conditions indicate that fatigue processes most probably operate in the field, with large *M. flaccida* fronds more susceptible to breakage by fatigue than small fronds and with female gametophytes more vulnerable and male gametophytes less vulnerable than tetrasporophytes.

DISCUSSION

Life history phase differences

The life history of *Mazzaella* consists of alternation of isomorphic generations: the haploid gametophyte phase alternates with the diploid tetrasporophyte phase, and gametophyte and tetrasporophyte fronds have similar overall morphology but differing reproductive structures. For *M. flaccida* and *M. splendens*, life history phase abundances vary over the species' geographical ranges, throughout the year, and with wave exposure of sites (Hansen and Doyle, 1976; Hansen, 1977; Foster, 1982; Dyck et al., 1985; DeWreede and Green, 1990; Dyck and DeWreede, 2006b).

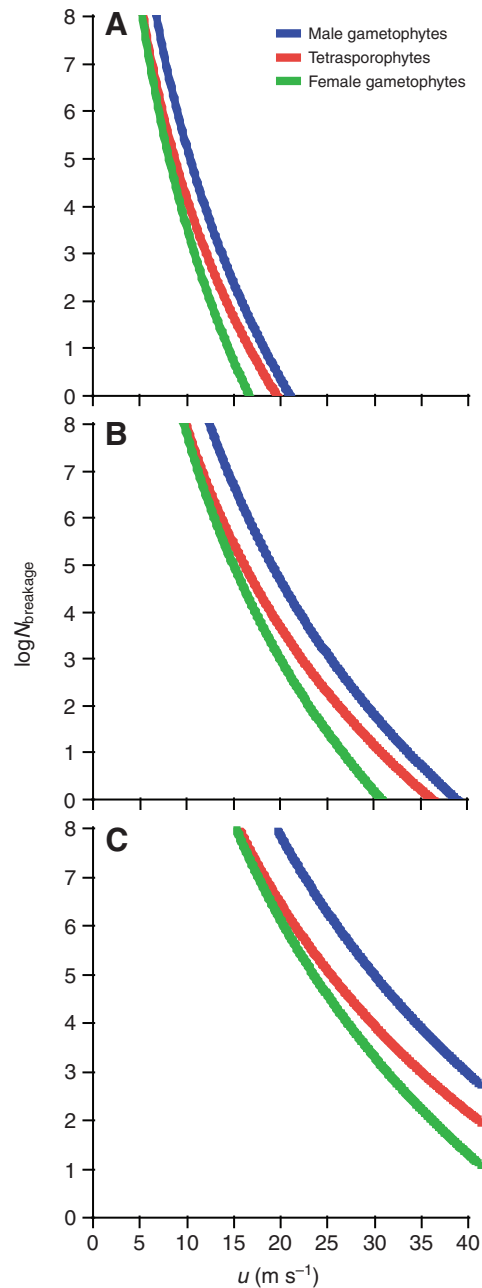


Fig. 12. Wave-imposed water velocities, u (m s^{-1}), versus number of loading cycles to breakage, N_{breakage} , for representative big (A), medium (B) and small (C) *M. flaccida* fronds. In each plot, the ordinate is logarithmic. Blue lines represent predictions for male gametophytes; red lines, tetrasporophytes; and green lines, female gametophytes.

Partially illuminating these contrasting life history phase abundances, some ecological differences have been identified for *M. splendens* gametophytes and tetrasporophytes (Dyck and DeWreede, 1995; Shaughnessy et al., 1996). For example, in one study, gametophytes changed their spatial density more rapidly than tetrasporophytes, attaining greater densities in spring and summer conditions and experiencing greater loss during fall and winter (Dyck and DeWreede, 1995). Experiments completed here point to biomechanical mechanisms, such as differences in fatigue behavior, that perhaps underpin such ecological patterns.

This study demonstrates clear mechanical strength differences among life history phases of *M. flaccida* and *M. splendens* (Fig. 3). Fatigue behavior measured here did demonstrate variability. However, similar variability has been observed in fatigue studies of other biological tissue when specimens originate from different individual organisms (Carter and Caler, 1983; Wren et al., 2003). For both *Mazzaella* species, tetrasporophytes displayed greater fatigue strengths than female gametophytes. (Fatigue strength is the repeated maximum stress that can be endured for a given number of loading cycles.) For *M. flaccida*, for which male gametophytes were also investigated, male gametophytes displayed greater fatigue strengths than tetrasporophytes and female gametophytes. Ecologically relevant differences have been suggested for heteromorphic phases of various macroalgae (Littler and Littler, 1980; Lubchenco and Cubit, 1980; Slocum, 1980; Dethier, 1981; Littler and Littler, 1983); results here additionally demonstrate mechanical differences, with potential ecological repercussions, across isomorphic phases of *M. flaccida* and *M. splendens*.

Only fronds that had become reproductive were used in this study. But some tetrasporophyte and female gametophyte test specimens did not possess reproductive structures. Examination of pull-to-break and fatigue strengths of these *M. splendens* specimens suggests that reproductive structures weaken specimens in both failure modes: pull-to-break and fatigue strengths were reduced in specimens with reproductive structures, which may cause elevated rates of breakage for reproductive fronds in the field. Along with frequent formation of cracks in and around *M. flaccida* female gametophyte cystocarps, these results for *M. splendens* point to mechanical costs of reproduction, which likely vary with life history phase.

In contrast, following *M. splendens* at one location, Dyck and DeWreede (Dyck and DeWreede, 2006a) found no change in survival probability following the onset of reproduction. However, consistent with my results, Dyck and DeWreede do suggest that the onset of reproduction may increase the likelihood of tearing and fragmentation of blades, even though dislodgment of entire fronds was not affected. My data and their observations together suggest that costs of reproduction may be tissue loss, not dislodgment of whole fronds or thalli.

Overall, demonstrated mechanical differences among *Mazzaella* life history phases and weakening associated with reproductive structures may influence survival rates and thus spatial and temporal variability in abundance across life history phases (e.g. Scrosati and DeWreede, 1999). Over evolutionary time, even slight differences among phases of isomorphic species are sufficient to produce and then maintain biphasic life cycles (Hughes and Otto, 1999). Furthermore, observed mechanical costs of reproductive structures may lead to tradeoffs between reproduction and breakage that potentially impact on life history evolution (Bell, 1984a; Bell, 1984b; Roff, 1992). For example, if they break more frequently during fall storms, female gametophyte fronds might experience selective pressure to reach reproductive maturity earlier in the year, at a younger age, compared with tetrasporophyte fronds. Finally, measured mechanical differences among life history phases may shape ecological interactions within *Mazzaella* populations by determining life history phase distributions or maximum frond sizes. For example, upon becoming reproductive, female gametophyte blades are more likely to tatter and break than tetrasporophyte and male gametophyte blades, perhaps imposing greater limitations to frond size or restricting distributions to more sheltered microhabitats.

Species differences

Mazzaella splendens was stronger in pull-to-break tests and in fatigue (Fig. 4). However, several potentially confounding factors in my comparison of *M. flaccida* and *M. splendens* must be considered. First, *M. flaccida* and *M. splendens* tests occurred in disparate geographical locations. *Mazzaella flaccida* was tested from central California populations in Monterey Bay, while *M. splendens* was tested from northern populations in the San Juan Islands, Washington. The pull-to-break and fatigue strengths of *M. flaccida* and *M. splendens* may differ over the species' geographical ranges. *M. flaccida* and *M. splendens* both occur from Alaska to Point Conception, CA, with populations following points of upwelling through Northern Baja California, Mexico (Abbott and Hollenberg, 1976), and no systematic attempt has been made here to quantify variation in mechanical properties over this latitudinal range. Second, *M. splendens* was collected from a floating dock in protected waters. Although its abundant growth on this structure facilitated the frequent collection required for experimental testing, *M. splendens* may exhibit different material properties in other habitats or on exposed coasts. Also, *M. splendens* from the protected floating dock likely had accumulated less fatigue damage prior to testing than *M. flaccida* from more exposed intertidal rocks, which may have improved measured fatigue behavior for *M. splendens*. Third, differing specimen sizes may have influenced measurements of fatigue strength. Specimen size sometimes influences measured material properties (Griffith, 1921; Wang and Ker, 1995). In the case of fatigue, larger specimens provide more area for, and thus may more readily experience, crack initiation. *M. flaccida* specimens were slightly larger, with cracks and failure originating in an unstretched specimen area of 2.4 cm². In contrast, the corresponding area for *M. splendens* was 1.8 cm². Fourth, loading profiles in fatigue tests differed between *M. flaccida* and *M. splendens*.

Nonetheless, as suggested by results from this study, *M. splendens* is most probably stronger than *M. flaccida* under both fatigue and pull-to-break loadings. *Mazzaella flaccida* generally has smaller blades and occupies higher intertidal locations than *M. splendens* (Abbott and Hollenberg, 1976). Observed strength differences may lead to disparities in frond size limits in the field, and potentially different breakage rates may influence ecological interactions between the species in low intertidal habitats where their distributions overlap.

Seasonal effects

Fatigue behavior of *M. flaccida* was assessed throughout the year (Fig. 5). No effect of season on fatigue behavior was observed, which contrasts with seasonal shifts in material properties demonstrated previously for several macroalgae (Johnson and Koehl, 1994; Pratt and Johnson, 2002). Growing and maturing rapidly (Hansen, 1977), *Mazzaella* varies in abundance throughout the year (Hansen, 1977; Foster, 1982; DeWreede and Green, 1990; Dyck and DeWreede, 2006b). Unlike engineering materials, living biological tissues, as in tendon, ligament and some macroalgae, can actively alter their material properties over time in response to changing mechanical loadings imposed *in situ* (Noyes, 1977; Norton et al., 1981; Armstrong, 1987; Woo et al., 1987; Kraemer and Chapman, 1991; Hayashi, 1996; Buchanan and Marsh, 2001; Kitzes and Denny, 2005; Arampatzis et al., 2007). Yet fatigue properties of *M. flaccida* apparently do not shift with seasonal fluctuations in wave-imposed forces. Instead, seasonal variations in *M. flaccida* abundance may result more from seasonal changes in wave-induced stresses and other physical factors than from seasonally weaker or stronger tissues.

Several qualifications are needed. Because fronds below a certain size were too small for me to cut specimens from, fatigue was not investigated in fronds of length under approximately 10 cm. Furthermore, only fronds that had become reproductive were tested. Finally, tattered fronds covered with holes were not used because all possible placements of the specimen template on such fronds would have created specimens with holes, which were avoided in this study of fatigue behavior in the absence of notches, cracks or holes. These very tattered fronds were likely the oldest and most senescent fronds in the population. Seasonal variations relating to small, non-reproductive or very tattered fronds remain unexplored.

Size effects

For *M. flaccida* and *M. splendens*, fatigue strength did not vary with frond length (Fig. 10) and likely did not vary greatly with frond age, given similar growth rates for individual fronds. A few other studies have found a similar lack of correlation between some measures of thallus size and mechanical strength (Carrington, 1990; Milligan and DeWreede, 2000; Pratt and Johnson, 2002).

Again, it should be noted that small fronds (less than approximately 10 cm in length) and very tattered fronds completely dotted with holes were not tested. Additionally, only fronds that had become reproductive were tested.

Thus, for all life history phases and species tested, fatigue strength remained constant over a large size and probably age range for reproductive fronds. Fatigue strength may differ in non-reproductive, small or very tattered fronds; the effects of such factors were not examined.

Crack formation

In general, fatigue failure consists of two parts: crack initiation and crack growth, the latter part eventually creating cracks long enough to fracture specimens. Here, for the first time, crack initiation was studied in the soft biological tissue of a macroalga, *Mazzaella*. In fatigue tests of *M. flaccida*, through photographic documentation I found that cracks formed relatively late, and grew more rapidly, compared with cracks in biological materials such as bone. For *M. flaccida*, as characterized by crack formation index *C* for first-visible cracks, approximately 80–90% of loading cycles required for fatigue failure were associated with crack initiation. That is, cracks appeared late, on average after 80–90% of the cycles required for fatigue failure had passed. Cracks then grew relatively quickly over the remaining 10–20% of total cycles, soon causing specimen fracture. Furthermore, the timing of crack formation differed across life history phases. Cracks formed later in male gametophytes than in female gametophytes and tetrasporophytes. Male gametophytes lack the distinct reproductive structures of female gametophytes and tetrasporophytes, which may have influenced the timing of crack formation.

On the other hand, in bone, one of the few biological materials for which crack initiation has been extensively investigated, microcracks form early, in approximately the first 10% of total life loading cycles (O'Brien et al., 2003). These cracks then generally cease growing upon encountering structural barriers such as cement lines (O'Brien et al., 2003; Taylor et al., 2007). Such structures thereby delay fatigue failure more than occurred in *M. flaccida* specimens.

For *M. flaccida*, morphology of fronds assumed a different role in fatigue failure. Instead of arresting crack growth, morphological structures contributed to the first part of fatigue, stimulating crack initiation. Endophytes in macroalgal fronds have been shown to reduce frond growth rates, to hinder some aspects of reproductive

output, and to decrease frond strength and survivorship (Apt, 1984; Correa et al., 1994; Buschmann et al., 1997; Faugeton et al., 2000). Here, endophytes, as well as cystocarp reproductive structures, were linked to crack formation. Cracks formed in association with endophytes and cystocarps significantly more often than expected by chance alone. In contrast to cystocarpic blades, tetrasporangial blades did not experience crack formation in association with tetrasporangial sori more often than would be expected by chance alone. This study thus demonstrates distinct and particular mechanical costs of endophytes and some reproductive structures: fronds hosting endophytes and female gametophytes bearing cystocarps are more susceptible to the formation of fatigue cracks.

Documentation of crack formation in association with specimens' lateral edges demonstrated that crack formation was not merely an artifact of specimen preparation. Approximately 18% of visible cracks formed along specimen edges. This percentage necessarily overestimated crack formation on specimen edges because some cracks may have formed away from specimen edges but grown to an edge by the time of photographic documentation. With 18% of cracks, or less, forming along specimen edges, I can thus conclude that my methods of preparing specimens for testing did not unduly influence crack formation. Most cracks (82%) formed away from the cut edges of specimens tested.

In *M. flaccida*, as in bone (Martin, 2003; O'Brien et al., 2003; Taylor et al., 2007), multiple cracks often formed. I focused on crack initiation and eventual failure, but more than one crack often formed between the appearance of the first crack and final fracture.

Time-dependent damage

Mazzaella blades consist of soft, viscoelastic tissue (Mach et al., 2007a; Mach et al., 2007b). They thus might be expected to display time-dependent damage [creep (*sensu* Carter and Caler, 1985; Caler and Carter, 1989)] in two aspects of this study: in loading frequency effects on fatigue and in elongation of specimens during fatigue tests.

Two types of damage may occur in viscoelastic materials subjected to repeated loadings: cycle-dependent and time-dependent damage. Cycle-dependent damage depends only on the maximum load applied in each loading cycle; it is fatigue damage as traditionally defined. Time-dependent damage is best explained by considering constant, non-varying loading of a material. When a constant load is applied to viscoelastic materials, inelastic creep strains will develop over time, sometimes leading to rupture. When viscoelastic materials are repeatedly loaded in fatigue tests, similar time-dependent damage, in addition to cycle-dependent damage, may occur. This time-dependent damage depends on the time spent at each level of loading, not just on maximum load applied in each cycle.

In some biological tissues, such as tendon, dentin and bone, time-dependent damage may contribute to failure in conditions of repeated loading (Caler and Carter, 1989; Wang et al., 1995; Bowman et al., 1998; Zioupos et al., 2001; Nalla et al., 2003; Nalla et al., 2005; Wren et al., 2003). As a result, loading frequency, leading to different total loading times and different amounts of time-dependent damage, sometimes influences or even determines fatigue behavior; that is, the number of cycles to failure for given repeatedly applied stresses (Caler and Carter, 1989; Wang et al., 1995; Zioupos et al., 2001; Nalla et al., 2003). Additionally, biological materials may develop creep strains upon repeated application of loadings in fatigue tests (Carter and Caler, 1983; Bowman et al., 1998; Wang et al., 1995; Wren et al., 2003).

For *M. flaccida*, loading frequency exerted only a modest influence on fatigue behavior, with specimens loaded at 2 Hz being slightly stronger than specimens loaded at 0.5 or 1 Hz (Fig. 6). Because there was a marginal effect of loading frequency, time-dependent damage may occur in *M. flaccida* to a small extent, in addition to cycle-dependent fatigue damage. Fatigue tests occurred over only a small range of loading frequencies because time limitations prevented testing at lower frequencies and because the large extensibility of specimens (engineering strain at breakage exceeding 0.5) made testing at higher loading frequencies impractical.

During fatigue tests, maximum strain of *M. flaccida* specimens increased over time, even though maximum imposed stress remained constant (Fig. 9). The proportional increases in strain for the first 20 loading cycles, described by S_{20} , were positively correlated with applied loading stress (Fig. 9B). In contrast, proportional increases in strain over entire fatigue tests, described by S_{entire} , were largely independent of repeatedly applied stress (Fig. 9C) but did vary with life history phase (Fig. 9D), with male gametophytes elongating in creep more than female gametophytes and tetrasporophytes.

Additionally, *M. flaccida* exhibited typical primary and secondary creep (e.g. Fig. 9A); tertiary creep was not observed (Hin and Cherry, 1984). That is, maximum strain in fatigue tests first increased at a decelerating rate (primary creep) and then increased at a constant rate (secondary creep) until specimen failure occurred. For polymers, bone and tendon, creep rate often rises rapidly prior to fracture (Carter and Caler, 1983; Carter and Caler, 1985; Caler and Carter, 1989; Bowman et al., 1994; Wang and Ker, 1995; Wren et al., 2003; Klompen et al., 2005; Ker, 2007), but this tertiary creep was not observed for *M. flaccida*.

Subsequent studies might further evaluate time-dependent damage in macroalgae, creating models to account for time-dependent and cycle-dependent damage (e.g. Carter and Caler, 1985; Caler and Carter, 1989; Wang and Ker, 1995; Wang et al., 1995; Wren et al., 2003), which may to some extent occur simultaneously in conditions of repeated loading. Repeated-loading fatigue tests were used as a starting point because seaweeds experience distinct, repeated loadings in the field – the action of wave after wave. A first priority was thus to assess fatigue behavior of *Mazzaella* in loading conditions resembling repeated wave-induced stresses. Further studies additionally should incorporate other characteristics of field hydrodynamic loadings, including pauses between waves, cessation of loading over the course of low tide, and different waveforms of imposed force, which vary across intertidal sites, dependent on substratum topography.

Implications for natural populations

Extrapolating observed crack growth rates to fronds without introduced cracks, Mach and colleagues (Mach et al., 2007b) concluded that fatigue operates over time scales relevant to macroalgae in the field. The results of the present fatigue study of *M. flaccida* strongly support this finding. Blades are predicted to break in loadings that may occur frequently during periods of high wave action (Fig. 12). For example, 50% of big, female gametophyte blades are expected to break in 54 loadings by wave-imposed velocities of 13 m s^{-1} , and 50% of big, tetrasporophyte blades should break in 354 loadings at 13 m s^{-1} . For 50% breakage, big, male gametophyte blades would require 2474 loadings at 13 m s^{-1} but only 242 loadings at 15 m s^{-1} . In the course of stormy periods, with over 8000 waves smashing the shore each day, water velocities under breaking waves likely cause big *M. flaccida* blades to fail by fatigue. Small *M. flaccida* blades are predicted to experience much less

fatigue breakage. For 50% breakage of the weakest life history phase, female gametophytes, over 1 million loadings at 20 m s^{-1} are predicted necessary, indicating that small blades are rarely at risk of fatigue failure. Medium-sized blades display fatigue failure risk that varies from low for female gametophytes to very low for male gametophytes: 50% of female gametophyte blades are predicted to break after 100,630 loadings at 15 m s^{-1} or after 1013 loadings at 20 m s^{-1} , while male gametophyte blades would require over 5 million loadings at 15 m s^{-1} or 48,443 loadings at 20 m s^{-1} .

These predictions of fatigue failure raise an obvious question: how often does *M. flaccida* experience velocities of 13, 15 or 20 m s^{-1} in the field? To date, water velocity measurement efforts have focused on maximum velocities (e.g. Helmuth and Denny, 2003). But for present purposes, all wave-imposed velocities, not just the maximum values, are of interest. Unfortunately, the frequencies with which *M. flaccida* encounters various wave-induced water velocities remain unknown.

In sum, fatigue failure of *M. flaccida* likely occurs at water velocities and over time scales actually experienced by fronds in the field. Risk of breakage is greatest for big fronds, which experience the largest wave-induced drag forces, and lowest for small fronds, which experience the smallest wave-imposed drag forces. Whereas big fronds probably break frequently during periods of large waves, small fronds are unlikely to break even when seas are stormy. This variation in breakage risk with frond size may explain observed limits to size in the intertidal region, the causes of which have been debated (Denny et al., 1985; Gaylord et al., 1994; Gaylord, 2000; Martone and Denny, 2008). Risk also varies with life history phase, with female gametophytes weaker than tetrasporophytes, which are weaker than male gametophytes.

The location of breakage in *Mazzaella* thalli warrants mention. The current study evaluated breakage of *Mazzaella* blades. There are other potential break locations: in stipes, at stipe–holdfast junctions, and at holdfast–substratum interfaces. Although initial examinations of *M. splendens*, in which investigators folded blades over experimental scale apparatuses and pulled on the macroalgae in the field, suggested breakage occurs primarily at stipe–holdfast junctions (Shaughnessy et al., 1996), subsequent measurements of wave-induced breakage found that fracture occurs within blades more often than at stipe–holdfast junctions (Shaughnessy and DeWreede, 2001). The current study thus evaluates a significant breakage location, the algal blade, but fracture may also happen elsewhere in *Mazzaella* thalli.

In engineering materials, fatigue damage accumulates until failure eventually occurs. Because macroalgae are composed of living tissues, fatigue failure is not necessarily an irremediable eventuality; biological repair can occur. Repair processes have been probed in biological materials such as bone and tendon (Schechtman and Bader, 1997; Ker, 1999; Ker et al., 2000; Martin, 2003; Taylor et al., 2007; Ker, 2008) and likely occur in *Mazzaella* as well. For example, slits introduced in *M. flaccida* blades have been shown to round at their tips within a few days (Denny et al., 1989), a form of repair that probably slows subsequent crack growth. Additionally, biological materials such as tendon can modulate their fatigue properties (Ker et al., 2000; Pike et al., 2000). However, *M. flaccida* is unlikely to be able to alter its fatigue strength in response to wave climate as its fatigue behavior does not change throughout the year (Fig. 5). Nonetheless, biological repair processes in *M. flaccida* probably occur, and they remain poorly understood. Periods of calm seas may allow repair of damage incurred during storms, for example, whereas repair may be less able to counteract fatigue damage in the midst of series of breaking waves.

Conclusion

This study indicates that failure by fatigue occurs in the seaweed *Mazzaella* in laboratory tests and in natural conditions. In the field, breakage due to fatigue is predicted to be greatest for large fronds and least for small fronds, potentially explaining limits to size observed for intertidal seaweeds. Furthermore, fatigue behavior varied substantially with life history phase. Overall, these results provide important insight into mechanical processes influencing the evolution and ecology of *Mazzaella*.

E. Carrington generously provided use of her equipment and laboratory for testing of *Mazzaella splendens*. M. Boller and L. Miller assisted with equipment preparation for drag coefficient measurements. M. Denny and D. Nelson provided critical advice and guidance in the design and presentation of this research. This manuscript benefited from the suggestions of J. Connor, L. Hunt, B. Grone, D. Mach, J. Mach, K. Miklasz and S. Tepler. In completion of this study, I received support from the Myers Oceanographic and Marine Biology Trust Grant, the Friday Harbor Laboratories Wainwright Fellowship, a Stanford Graduate Fellowship, and a Stanford Interdisciplinary Graduate Fellowship.

LIST OF ABBREVIATIONS

A	representative frond area (single-sided surface area), Eqn 4
C	crack formation index, Eqn 1
C_D	drag coefficient, Eqn 4
F_D	drag force, Eqn 4
L_{frond}	frond length
N_{breakage}	number of cycles to breakage, Eqn 1
$N_{\text{breakage,predicted}}$	number of cycles to breakage predicted from regression equations
$N_{\text{crack formation}}$	number of cycles to crack formation, Eqn 1
r	residual for actual <i>versus</i> predicted loading cycles to breakage
S_{20}	strain change index for first 20 loading cycles, Eqn 2
S_{entire}	strain change index for entire fatigue tests, Eqn 3
u	water velocity, Eqn 4
$\epsilon_{\text{max,initial}}$	maximum strain in first loading cycle, Eqn 2
$\epsilon_{\text{max,20}}$	maximum strain in 20th loading cycle, Eqn 2
$\epsilon_{\text{max,final}}$	maximum strain at end of fatigue test, Eqn 3
ρ	fluid density, Eqn 4
σ_{max}	maximum stress imposed in each loading cycle

REFERENCES

- Abbot, I. A. and Hollenberg, G. J. (1976). *Marine Algae of California*. Stanford, CA: Stanford University Press.
- Apt, K. E. (1984). Effects of the symbiotic red alga *Hypneocolax stellaris* on its host *Hypnea musciformis* (Hypneaceae, Gigartinales). *J. Phycol.* **20**, 148-150.
- Arampatzis, A., Karamanidis, K. and Albracht, K. (2007). Adaptational responses of the human Achilles tendon by modulation of the applied cyclic strain magnitude. *J. Exp. Biol.* **210**, 2743-2753.
- Armstrong, S. L. (1987). Mechanical properties of the tissues of the brown alga *Hedophyllum sessile* (C. Ag.) Setchell: variability with habitat. *J. Exp. Mar. Biol. Ecol.* **114**, 143-151.
- Baskerville, G. L. (1972). Use of logarithmic regression in the estimation of plant biomass. *Can. J. For. Res.* **2**, 49-53.
- Beauchamp, J. J. and Olson, J. S. (1973). Corrections for bias in regression estimates after logarithmic transformation. *Ecology* **54**, 1403-1407.
- Bell, G. (1984a). Measuring the cost of reproduction. I. The correlation structure of the life table of a plankton rotifer. *Evolution* **38**, 300-313.
- Bell, G. (1984b). Measuring the cost of reproduction. II. The correlation structure of the life tables of five freshwater invertebrates. *Evolution* **38**, 314-326.
- Black, R. (1976). The effects of grazing by the limpet, *Acmaea insessa*, on the kelp, *Egregia laevigata*, in the intertidal zone. *Ecology* **57**, 265-277.
- Blanchette, C. A. (1997). Size and survival of intertidal plants in response to wave action: a case study with *Fucus gardneri*. *Ecology* **78**, 1563-1578.
- Boller, M. L. and Carrington, E. (2006a). *In situ* measurements of hydrodynamic forces imposed on *Chondrus crispus* Stackhouse. *J. Exp. Mar. Biol. Ecol.* **337**, 159-170.
- Boller, M. L. and Carrington, E. (2006b). The hydrodynamic effects of shape and size change during reconfiguration of a flexible macroalga. *J. Exp. Biol.* **209**, 1894-1903.
- Bowman, S. M., Keaveny, T. M., Gibson, L. J., Hayes, W. C. and McMahon, T. A. (1994). Compressive creep behavior of bovine trabecular bone. *J. Biomech.* **27**, 301-310.
- Bowman, S. M., Guo, X. E., Cheng, D. W., Keaveny, T. M., Gibson, L. J., Hayes, W. C. and McMahon, T. A. (1998). Creep contributes to the fatigue behavior of bovine trabecular bone. *J. Biomech. Eng.* **120**, 647-654.
- Buchanan, C. I. and Marsh, R. L. (2001). Effects of long-term exercise on the biomechanical properties of the Achilles tendon of guinea fowl. *J. Appl. Physiol.* **90**, 164-171.
- Buschmann, A. H., Correa, J. A., Beltrán, J. and Retamales, C. A. (1997). Determinants of disease expression and survival of infected individual fronds in wild populations of *Mazzaella laminarioides* (Rhodophyta) in central and southern Chile. *Mar. Ecol. Prog. Ser.* **154**, 269-280.
- Caler, W. E. and Carter, D. R. (1989). Bone creep-fatigue damage accumulation. *J. Biomech.* **22**, 625-635.
- Carrington, E. (1990). Drag and dislodgment of an intertidal macroalga: consequences of morphological variation in *Mastocarpus papillatus* Kützinger. *J. Exp. Mar. Biol. Ecol.* **139**, 185-200.
- Carrington, E., Grace, S. P. and Chopin, T. (2001). Life history phases and the biomechanical properties of the red alga *Chondrus crispus* (Rhodophyta). *J. Phycol.* **37**, 699-704.
- Carter, D. R. and Caler, W. E. (1983). Cycle-dependent and time-dependent bone fracture with repeated loading. *J. Biomech. Eng.* **105**, 166-170.
- Carter, D. R. and Caler, W. E. (1985). A cumulative damage model for bone fracture. *J. Orthop. Res.* **3**, 84-90.
- Choi, K. and Goldstein, S. A. (1992). A comparison of the fatigue behavior of human trabecular and cortical bone tissue. *J. Biomech.* **25**, 1371-1381.
- Chopin, T., Kerin, B. F. and Mazerolle, R. (1999). Phyccocolloid chemistry as a taxonomic indicator of phylogeny in the Gigartinales, Rhodophyceae: a review and current developments using Fourier transform infrared diffuse reflectance spectroscopy. *Phycol. Res.* **47**, 167-188.
- Correa, J. A., Flores, V. and Garrido, J. (1994). Green patch disease in *Iridaea laminarioides* (Rhodophyta) caused by *Endophyton* sp. (Chlorophyta). *Dis. Aquat. Org.* **19**, 203-213.
- Craigie, J. S. (1990). Cell walls. In *Biology of the Red Algae* (ed. K. M. Cole and R. G. Sheath), pp. 221-257. Cambridge: Cambridge University Press.
- Denny, M. W. (2006). Ocean waves, nearshore ecology, and natural selection. *Aquat. Ecol.* **40**, 439-461.
- Denny, M. and Gaylord, B. (2002). The mechanics of wave-swept algae. *J. Exp. Biol.* **205**, 1355-1362.
- Denny, M. and Wetthey, D. (2001). Physical processes that generate patterns in marine communities. In *Marine Community Ecology* (ed. M. D. Bertness, S. D. Gaines, and M. E. Hay), pp. 3-37. Sunderland: Sinauer Associates.
- Denny, M. W., Daniel, T. L. and Koehl, M. A. R. (1985). Mechanical limits to size in wave-swept organisms. *Ecol. Monogr.* **55**, 69-102.
- Denny, M., Brown, V., Carrington, E., Kraemer, G. and Miller, A. (1989). Fracture mechanics and the survival of wave-swept macroalgae. *J. Exp. Mar. Biol. Ecol.* **127**, 211-228.
- Denny, M. W., Gaylord, B. P. and Cowen, E. A. (1997). Flow and flexibility: II. The roles of size and shape in determining wave forces on the bull kelp *Nereocystis luetkeana*. *J. Exp. Biol.* **200**, 3165-3183.
- Dethier, M. N. (1981). Heteromorphic algal life histories: the seasonal pattern and response to herbivory of the brown crust, *Ralfsia californica*. *Oecologia* **49**, 333-339.
- DeWreede, R. E. and Green, L. G. (1990). Patterns of gametophyte dominance of *Iridaea splendens* (Rhodophyta) in Vancouver Harbour, Vancouver, British Columbia, Canada. *J. Appl. Phycol.* **2**, 27-34.
- Dudgeon, S. R. and Johnson, A. S. (1992). Thick vs. thin: thallus morphology and tissue mechanics influence differential drag and dislodgment of two co-dominant seaweeds. *J. Exp. Mar. Biol. Ecol.* **165**, 23-43.
- Dudgeon, S. R., Steneck, R. S., Davison, I. R. and Vadas, R. L. (1999). Coexistence of similar species in a space-limited intertidal zone. *Ecol. Monogr.* **69**, 331-352.
- Dyck, L. J. and DeWreede, R. E. (1995). Patterns of seasonal demographic change in the alternate isomorphic stages of *Mazzaella splendens* (Gigartinales, Rhodophyta). *Phycologia* **34**, 390-395.
- Dyck, L. J. and DeWreede, R. E. (2006a). Reproduction and survival in *Mazzaella splendens* (Gigartinales, Rhodophyta). *Phycologia* **45**, 302-310.
- Dyck, L. J. and DeWreede, R. E. (2006b). Seasonal and spatial patterns of population density in the marine macroalga *Mazzaella splendens* (Gigartinales, Rhodophyta). *Phycol. Res.* **54**, 21-31.
- Dyck, L., DeWreede, R. E. and Garbary, D. (1985). Life history phases in *Iridaea cordata* (Gigartinales): relative abundance and distribution from British Columbia to California. *Jap. J. Phycol.* **33**, 225-232.
- Faugeron, S., Martínez, E. A., Sánchez, P. A. and Correa, J. A. (2000). Infectious diseases in *Mazzaella laminarioides* (Rhodophyta): estimating the effect of infections on host reproductive potential. *Dis. Aquat. Org.* **42**, 143-148.
- Foster, M. S. (1982). Factors controlling the intertidal zonation of *Iridaea flaccida* (Rhodophyta). *J. Phycol.* **18**, 285-294.
- Friedland, M. T. and Denny, M. W. (1995). Surviving hydrodynamic forces in a wave-swept environment: consequences of morphology in the feather boa kelp, *Egregia menziesii* (Turner). *J. Exp. Mar. Biol. Ecol.* **190**, 109-133.
- Gaylord, B. (1999). Detailing agents of physical disturbance: wave-induced velocities and accelerations on a rocky shore. *J. Exp. Mar. Biol. Ecol.* **239**, 85-124.
- Gaylord, B. (2000). Biological implications of surf-zone flow complexity. *Limnol. Oceanogr.* **45**, 174-188.
- Gaylord, B. and Denny, M. W. (1997). Flow and flexibility: I. Effects of size, shape and stiffness in determining wave forces on the stipitate kelps *Eisenia arborea* and *Pterygophora californica*. *J. Exp. Biol.* **200**, 3141-3164.
- Gaylord, B., Blanchette, C. A. and Denny, M. W. (1994). Mechanical consequences of size in wave-swept algae. *Ecol. Monogr.* **64**, 287-313.
- Griffith, A. A. (1921). The phenomena of rupture and flow in solids. *Philos. Trans. R. Soc. Lond. A* **221**, 163-198.
- Hale, B. (2001). Macroalgal materials: foiling fracture and fatigue from fluid forces. PhD Thesis, Stanford University, Stanford, CA, USA.
- Hansen, J. E. (1977). Ecology and natural history of *Iridaea cordata* (Gigartinales, Rhodophyta) growth. *J. Phycol.* **13**, 395-402.
- Hansen, J. E. and Doyle, W. T. (1976). Ecology and natural history of *Iridaea cordata* (Rhodophyta; Gigartinales): population structure. *J. Phycol.* **12**, 273-278.
- Hawes, I. and Smith, R. (1995). Effect of current velocity on the detachment of thalli of *Ulva lactuca* (Chlorophyta) in a New Zealand estuary. *J. Phycol.* **31**, 875-880.

- Hayashi, K. (1996). Biomechanical studies of the remodeling of knee joint tendons and ligaments. *J. Biomech.* **29**, 707-716.
- Hearle, J. W. S. (1967). Fatigue in fibres and plastics (a review). *J. Mater. Sci.* **2**, 474-488.
- Helmuth, B. and Denny, M. W. (2003). Predicting wave exposure in the rocky intertidal zone: do bigger waves always lead to larger forces? *Limnol. Oceanogr.* **48**, 1338-1345.
- Hin, T. S. and Cherry, B. W. (1984). Creep rupture of a linear polyethylene: 1. Rupture and pre-rupture phenomena. *Polymer* **25**, 727-734.
- Hughes, J. S. and Otto, S. P. (1999). Ecology and the evolution of biphasic life cycles. *Am. Nat.* **154**, 306-320.
- Johnson, A. S. (2001). Drag, drafting, and mechanical interactions in canopies of the red alga *Chondrus crispus*. *Biol. Bull.* **201**, 126-135.
- Johnson, A. S. and Koehl, M. A. R. (1994). Maintenance of dynamic strain similarity and environmental stress factor in different flow habitats: thallus allometry and material properties of a giant kelp. *J. Exp. Biol.* **195**, 381-410.
- Ker, R. F. (1999). The design of soft collagenous load-bearing tissues. *J. Exp. Biol.* **202**, 3315-3324.
- Ker, R. F. (2007). Mechanics of tendon, from an engineering perspective. *Int. J. Fatigue* **29**, 1001-1009.
- Ker, R. F. (2008). Damage and fatigue. In *Collagen: Structure and Mechanics* (ed. P. Fratzl), pp. 111-131. New York: Springer Science and Business Media.
- Ker, R. F., Wang, X. T. and Pike, A. V. L. (2000). Fatigue quality of mammalian tendons. *J. Exp. Biol.* **203**, 1317-1327.
- Kitzes, J. A. and Denny, M. W. (2005). Red algae respond to waves: morphological and mechanical variation in *Mastocarpus papillatus* along a gradient of force. *Biol. Bull.* **208**, 114-119.
- Kloareg, B. and Quatrano, R. S. (1988). Structure of the cell walls of marine algae and ecophysiological functions of the matrix polysaccharides. *Oceanogr. Mar. Biol. Annu. Rev.* **26**, 259-315.
- Klumpen, E. T. J., Engels, T. A. P., van Breemen, L. C. A., Schreurs, P. J. G., Govaert, L. E. and Meijer, H. E. H. (2005). Quantitative prediction of long-term failure of polycarbonate. *Macromolecules* **38**, 7009-7017.
- Koehl, M. A. R. (1984). How do benthic organisms withstand moving water? *Am. Zool.* **24**, 57-70.
- Koehl, M. A. R. (1986). Seaweeds in moving water: form and mechanical function. In *On the Economy of Plant Form and Function* (ed. T. J. Givnish), pp. 603-634. Cambridge: Cambridge University Press.
- Koehl, M. A. R. and Alberte, R. S. (1988). Flow, flapping, and photosynthesis of *Nereocystis luetkeana*: a functional comparison of undulate and flat blade morphologies. *Mar. Biol.* **99**, 435-444.
- Kraemer, G. P. and Chapman, D. J. (1991). Biomechanics and alginic acid composition during hydrodynamic adaptation by *Egregia menziesii* (Phaeophyta) juveniles. *J. Phycol.* **27**, 47-53.
- Littler, M. M. and Littler, D. S. (1980). The evolution of thallus form and survival strategies in benthic marine macroalgae: field and laboratory tests of a functional form model. *Am. Nat.* **116**, 25-44.
- Littler, M. M. and Littler, D. S. (1983). Heteromorphic life-history strategies in the brown alga *Scytosiphon lomentaria* (Lyngb.) Link. *J. Phycol.* **19**, 425-431.
- Lubchenco, J. and Cubitt, J. (1980). Heteromorphic life histories of certain marine algae as adaptations to variations in herbivory. *Ecology* **61**, 676-687.
- Mach, K. J., Nelson, D. V. and Denny, M. W. (2007a). Review: techniques for predicting the lifetimes of wave-swept macroalgae: a primer on fracture mechanics and crack growth. *J. Exp. Biol.* **210**, 2213-2230.
- Mach, K. J., Hale, B. B., Denny, M. W. and Nelson, D. V. (2007b). Death by small forces: a fracture and fatigue analysis of wave-swept macroalgae. *J. Exp. Biol.* **210**, 2231-2243.
- Martin, R. B. (2003). Fatigue microdamage as an essential element of bone mechanics and biology. *Calcif. Tissue Int.* **73**, 101-107.
- Martone, P. T. and Denny, M. W. (2008). To break a coralline: mechanical constraints on the size and survival of a wave-swept seaweed. *J. Exp. Biol.* **211**, 3433-3441.
- Miller, L. P. and Gaylord, B. (2007). Barriers to flow: the effects of experimental cage structures on water velocities in high-energy subtidal and intertidal environments. *J. Exp. Mar. Biol. Ecol.* **344**, 215-228.
- Milligan, K. L. D. and DeWreede, R. E. (2000). Variations in holdfast attachment mechanics with developmental stage, substratum-type, season, and wave-exposure for the intertidal kelp species *Hedophyllum sessile* (C. Agardh) Setchell. *J. Exp. Mar. Biol. Ecol.* **254**, 189-209.
- Nalla, R. K., Imbeni, V., Kinney, J. H., Staninec, M., Marshall, S. J. and Ritchie, R. O. (2003). *In vitro* fatigue behavior of human dentin with implications for life prediction. *J. Biomed. Mater. Res.* **66A**, 10-20.
- Nalla, R. K., Kruzic, J. J., Kinney, J. H. and Ritchie, R. O. (2005). Aspects of *in vitro* fatigue in human cortical bone: time and cycle dependent crack growth. *Biomaterials* **26**, 2183-2195.
- Norton, T. A., Mathieson, A. C. and Neushul, M. (1981). Morphology and environment. In *The Biology of Seaweeds* (ed. C. S. Lobban and M. J. Wynne), pp. 421-451. Berkeley, CA: University of California Press.
- Noyes, F. R. (1977). Functional properties of knee ligaments and alterations induced by immobilization: a correlative biomechanical and histological study in primates. *Clin. Orthop. Relat. Res.* **123**, 210-242.
- O'Brien, F. J., Taylor, D. and Lee, T. C. (2003). Microcrack accumulation at different intervals during fatigue testing of compact bone. *J. Biomech.* **36**, 973-980.
- Pike, A. V. L., Ker, R. F. and Alexander, R. M. (2000). The development of fatigue quality in high- and low-stressed tendons of sheep (*Ovis aries*). *J. Exp. Biol.* **203**, 2187-2193.
- Pratt, M. C. and Johnson, A. S. (2002). Strength, drag, and dislodgment of two competing intertidal algae from two wave exposures and four seasons. *J. Exp. Mar. Biol. Ecol.* **272**, 71-101.
- Roff, D. A. (1992). *The Evolution of Life Histories: Theory and Analysis*. New York: Chapman & Hall.
- Schechtman, H. and Bader, D. L. (1997). *In vitro* fatigue of human tendons. *J. Biomech.* **30**, 829-835.
- Scrosati, R. and DeWreede, R. E. (1999). Demographic models to simulate the stable ratio between ecologically similar gametophytes and tetrasporophytes in populations of the Gigartinales (Rhodophyta). *Phycol. Res.* **47**, 153-157.
- Seymour, R. J., Tegner, M. J., Dayton, P. K. and Parnell, P. E. (1989). Storm wave induced mortality of giant kelp, *Macrocystis pyrifera*, in Southern California. *Estuar. Coast. Shelf Sci.* **28**, 277-292.
- Shaughnessy, F. J. and DeWreede, R. E. (2001). Size, survival and the potential for reproduction in transplants of *Mazzaella splendens* and *M. linearis* (Rhodophyta). *Mar. Ecol. Prog. Ser.* **222**, 109-118.
- Shaughnessy, F. J., DeWreede, R. E. and Bell, E. C. (1996). Consequences of morphology and tissue strength to blade survivorship of two closely related Rhodophyta species. *Mar. Ecol. Prog. Ser.* **136**, 257-266.
- Slocum, C. J. (1980). Differential susceptibility to grazers in two phases of an intertidal alga: advantages of heteromorphic generations. *J. Exp. Mar. Biol. Ecol.* **46**, 99-110.
- Sprugel, D. G. (1983). Correcting for bias in log-transformed allometric equations. *Ecology* **64**, 209-210.
- Stephens, R. I., Fateni, A., Stephens, R. R. and Fuchs, H. O. (2001). *Metal Fatigue in Engineering*. 2nd edn. New York: J. Wiley.
- Taylor, D., Hazenberg, J. G. and Lee, T. C. (2007). Living with cracks: damage and repair in human bone. *Nat. Mater.* **6**, 263-268.
- Tomanek, L. and Helmuth, B. (2002). Physiological ecology of rocky intertidal organisms: a synergy of concepts. *Int. Comp. Biol.* **42**, 771-775.
- Utter, B. D. and Denny, M. W. (1996). Wave-induced forces on the giant kelp *Macrocystis pyrifera* (Agardh): field test of a computational model. *J. Exp. Biol.* **199**, 2645-2654.
- Vogel, S. (1984). Drag and flexibility in sessile organisms. *Am. Zool.* **24**, 37-44.
- Wang, X. T. and Ker, R. F. (1995). Creep rupture of wallaby tail tendons. *J. Exp. Biol.* **198**, 831-845.
- Wang, X. T., Ker, R. F. and Alexander, R. M. (1995). Fatigue rupture of wallaby tail tendons. *J. Exp. Biol.* **198**, 847-852.
- Woo, S. L. Y., Gomez, M. A., Sites, T. J., Newton, P. O., Orlando, C. A. and Akeson, W. H. (1987). The biomechanical and morphological changes in the medial collateral ligament of the rabbit after immobilization and remobilization. *J. Bone Joint Surg.* **69-A**, 1200-1211.
- Wren, T. A. L., Lindsey, D. P., Beaupré, G. S. and Carter, D. R. (2003). Effects of creep and cyclic loading on the mechanical properties and failure of human Achilles tendon. *Ann. Biomed. Eng.* **31**, 710-717.
- Zioupou, P. and Currey, J. D. (1994). The extent of microcracking and the morphology of microcracks in damaged bone. *J. Mater. Sci.* **29**, 978-986.
- Zioupou, P., Wang, X. T. and Currey, J. D. (1996). The accumulation of fatigue microdamage in human cortical bone of two different ages. *Clin. Biomech.* **11**, 365-375.
- Zioupou, P., Currey, J. D. and Casinos, A. (2001). Tensile fatigue in bone: are cycles, or time to failure, or both, important? *J. Theor. Biol.* **210**, 389-399.